Integral equation methods for elastance and mobility problems in two dimensions

Manas Rachh [*]   L. Greengard [†]

November 6, 2018

Abstract

We present new integral representations in two dimensions for the elastance problem in electrostatics and the mobility problem in Stokes flow. These representations lead to resonance-free Fredholm integral equations of the second kind and well conditioned linear systems upon discretization. By coupling our integral equations with high order quadrature and fast multipole acceleration, large-scale problems can be solved with only modest computing resources. We also discuss some applications of these boundary value problems in applied physics.

1   Introduction

A classical problem in electrostatics is the analysis of capacitance. Briefly stated, for an *open* system in two dimensions, this concerns a collection of N disjoint, bounded regions, denoted by D_j, with boundaries Γ_j, all of which are assumed to be perfect conductors. Setting the potential (the voltage) on the jth conductor to ϕ_j for $j = 1, \ldots, N$, one would like to determine the net charge q_j which accumulates on the conductors D_j for $j = 1, \ldots, N$. Since electrostatics is governed by a linear partial differential equation (the Laplace equation), there is a matrix, denoted by $\mathbf{C}$, such that

$$\mathbf{q} = \mathbf{C}\,\boldsymbol{\phi}\,, \tag{1}$$

where $\boldsymbol{\phi} = (\phi_1, \ldots, \phi_N)$ and $\mathbf{q} = (q_1, \ldots, q_N)$. The matrix $\mathbf{C}$ is referred to as the *capacitance matrix*.

Less well-studied is the converse problem, where a fixed amount of charge is placed on each of the N conductors, and the goal is to determine the corresponding, unknown, potentials. The matrix corresponding to that mapping is

---
[*]Courant Institute of Mathematical Sciences, New York University. New York, NY 10012-1110. (`rachh@cims.nyu.edu`).

[†]Simons Foundation and Courant Institute of Mathematical Sciences, New York University. (`greengard@cims.nyu.edu`).

called the *elastance matrix* [1], denote by $\mathbf{P}$, with

$$\phi = \mathbf{P}\,\mathbf{q}\,.$$

We should note that the goal is achievable, since the voltage on a perfect conductor is constant from Maxwell's equations [2]. $\mathbf{P}$ is the inverse of $\mathbf{C}$, in a suitably-defined space, discussed in greater detail in the next section. Given either the capacitance or elastance matrix, it is straightforward to compute the electrostatic energy E of the system [2], since

$$E = \frac{1}{2}\phi^T \mathbf{q} = \frac{1}{2}\phi^T \mathbf{C}\phi = \frac{1}{2}\mathbf{q}^T \mathbf{P}\mathbf{q}\,.$$

In some contexts, particularly in chip design, the capacitance problem is more typical [3, 4, 5, 6]. In others, including some quantum mechanical settings, the elastance problem arises more naturally [7, 8, 9]. The elastance matrix is sometimes referred to as the charging energy matrix.

A similar duality exists in problems of Stokes flow. Given N disjoint, rigid bodies, denoted by D_i, with boundaries Γ_i, with prescribed translational and rotational velocities, $(\mathbf{v}_i, \omega_i)$, the *resistance problem* consists of determing the corresponding forces and torques $(\mathbf{F}_i, T_i)$ on each of the bodies. The *mobility problem* is the reverse; given prescribed forces and torques on each of the rigid bodies, find the corresponding velocities (see, for example, [10, 11, 12, 13]). The mappings $\mathbf{R}$ and $\mathbf{M}$ such that

$$\overline{\mathbf{F}} = \mathbf{R}\,\overline{\mathbf{U}} \quad \text{and} \quad \overline{\mathbf{U}} = \mathbf{M}\,\overline{\mathbf{F}}$$

are known as the resistance and mobility tensors. Here, $\overline{\mathbf{U}} = (\mathbf{v}_1, \omega_1, \ldots, \mathbf{v}_N, \omega_N)$ and $\overline{\mathbf{F}} = (\mathbf{F}_1, T_1, \ldots, \mathbf{F}_N, T_N)$.

Reformulating the governing partial differential equation as a boundary integral equation is a natural approach for the above problems, since this reduces the dimensionality of the problem (discretizing the boundaries Γ_i alone) and permits high order accuracy to be achieved in complicated geometries. Moreover, boundary integral equations can be solved in optimal or nearly optimal time using suitable fast algorithms [14, 15, 16, 17], and satisfy the far field boundary conditions necessary to model an open system without the need for artificial truncation of the computational domain.

In this paper, we will restrict our attention largely to the formulation of suitable integral equations for the elastance and mobility problems. There is a substantial literature on the development of well-conditioned second-kind Fredholm equations to address the capacitance problem, which we do not seek to review here. We simply note that to apply $\mathbf{C}$ to a vector ϕ is equivalent (in the two-dimensional setting) to solving the Dirichlet problem:

$$\Delta u(\mathbf{x}) = 0 \quad \mathbf{x} \in \mathbb{R}^2 \setminus \left(\cup_{i=1}^{N} \overline{D_i} \right) \tag{2}$$

$$u|_{\Gamma_j} = \phi_j\,, \tag{3}$$

together with the radiation condition that $u(\mathbf{x})$ be bounded as $|\mathbf{x}| \to \infty$. The boundedness of $u(\mathbf{x})$ enforces charge neutrality on the collection of conductors. To see this, note that standard multipole estimates imply that

$$u(\mathbf{x}) \to C + \frac{Q}{2\pi} \log |\mathbf{x}|$$

as $|\mathbf{x}| \to \infty$, where C is constant and Q is the net charge induced on all the conductors. Thus, there would be logarithmic growth of the potential at infinity if the system were not charge neutral.

Remark 1. *It is worth noting that the constant C cannot be specified independently. If, for example, ϕ_j were set to 1 on all conductors, the solution to the Dirichlet problem must be $u(\mathbf{x}) = 1$ (under the assumption of charge neutrality), so that $C = 1$.*

The Dirichlet problem, as noted above, is well-known to have a unique solution and a variety of well-conditioned integral equations have been derived for its solution (see [5, 18, 19, 20, 21] and the references therein). The resistance problem involves solving the Stokes equations with boundary conditions imposed on the velocity, for which there are, again, a large number of well-conditioned formulations [12, 13, 22, 23, 24]. Suitable integral representations have been developed for both the elastance and mobility problems, often in the form of first kind integral equations [25] or second kind integral equations with N additional unknowns and N additional constraints [26]. While these have been shown to be very effective, when N is large and the geometry is complex, it is advantageous to work with formulations that are both well-conditioned (formulated as second kind boundary integral equations) and free of additional unknowns and constraints. We develop such an approach for the electrostatic problem first, in section 2, followed by the Stokes mobility problem in section 3. We illustrate their effectiveness with numerical examples in section 4 and discuss generalizations in section 5.

Remark 2. *We note that the elastance problem can be interpreted as a special case of a modified Dirichlet problem, and second kind Fredholm integral equations for the modified Dirichlet problem are developed and discussed in [20]. In our representation, we compute the physical charge density on each conductor directly and stably. For the representation discussed in [20], the charge density is given in terms of a hypersingular integral.*

Second kind integral equations for mobility problems without additional constraints were developed earlier by Kim and Karrila [27], using the Lorentz reciprocal identity. Our derivation, which leads to essentially the same integral equation, is direct - based on the physical principle that the interior of a rigid body must be stress free. Finally, the mobility problem can also be solved using a double layer representation without additional unknowns. For a detailed discussion of this representation, we refer the reader to [13, 28]. Our formulation has the advantage that certain derivative quantities, such as fluid stresses, can be computed with weakly singular instead of hypersingular kernels.

2   The Elastance Problem

Given the set of conductors $\{D_i\}_{i=1}^N$, let us assume that the boundaries $\Gamma_i = \partial D_i$ are positively oriented. We will denote by Γ the total boundary $\Gamma = \cup_{i=1}^N \Gamma_i$ and by $\mathbf{n_x}$ the outward normal at $\mathbf{x} \in \Gamma$. We let $E = \mathbb{R}^2 \setminus \left(\cup_{i=1}^N \overline{D_i} \right)$ denote the exterior domain. For the sake of simplicty, we assume that the conductors have smooth boundaries (Fig. 1.)
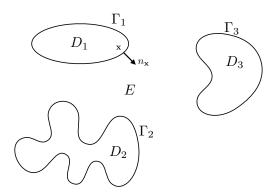

Figure 1: Three, smooth bounded conductors in the plane, with the exterior domain denoted by E. For $\mathbf{x}$ on the boundary, $\mathbf{n_x}$ represents the outward normal.

Application of the elastance matrix to a vector of charge strengths $\mathbf{q} = (q_1, q_2 \ldots q_N)$ is equivalent to the solution of the following boundary value problem for the potential $u(\mathbf{x})$ in the exterior domain E:

$$\Delta u(\mathbf{x}) = 0 \qquad \mathbf{x} \in E \tag{4}$$

$$u|_{\Gamma_j} = \phi_j \tag{5}$$

$$-\int_{\Gamma_j} \frac{\partial u}{\partial n} ds_{\mathbf{x}} = q_j \tag{6}$$

$$u(\mathbf{x}) \to 0 \quad \text{as } |\mathbf{x}| \to \infty. \tag{7}$$

Here, $u(\mathbf{x})$ and the constants $\{\phi_j\}_{j=1}^N$ are unknown. As noted in the introduction, it is a consequence of the Maxwell equations that the potential on each distinct conducting surface is constant, so that the boundary condition (5) corresponds to the physical problem of interest. (6) enforces the desired charging of the individual conductors, and (7) corresponds to setting the potential at infinity to zero (ground).

Remark 3. *(**Charge neutrality**): It is often said that the elastance matrix* $\mathbf{P}$ *is the inverse of the capacitance matrix* $\mathbf{C}$. *Unfortunately, it is straightforward to verify that, for the vector of potential values* $\boldsymbol{\phi}_0 = (1, \ldots, 1)$, *we have* $\mathbf{C}\boldsymbol{\phi}_0 = 0$, *so that* $\mathbf{C}$ *is not actually invertible. Likewise, the elastance boundary value*

problem, as stated above, cannot be solved unless $\mathbf{q} = (q_1, q_2 \ldots q_N)$ *satisfies*

$$\sum_{j=1}^{N} q_j = 0. \tag{8}$$

Otherwise, $u(\mathbf{x})$ *would have logarithmic growth at infinity. That is the sense in which* $\mathbf{P}$ *is the inverse of* $\mathbf{C}$ *- as a map defined on the space of mean zero vectors in* $\mathbb{R}^N$.

To prove uniqueness for the elastance problem, we will need the following lemma [29].

Lemma 1. *Let* u *be a harmonic function in the exterior domain* E *defined above, satisfying the condition* (7). *Let* $B_R(0)$ *be the ball of radius* R *centered at the origin and let* $\partial B_R(0)$ *be its boundary. Then, there exist* M, R_0 *such that* $\sup_{\partial B_R(0)} |\nabla u| \leq \frac{M}{R^2}$ *for all* $R \geq R_0$.

Lemma 2. *(Uniqueness). Suppose that* u *satisfies equations* (4), (5), (6) *and* (7), *with* $q_i = 0$ *for* $i = 1, \ldots, N$. *Then,* $u(\mathbf{x}) \equiv 0$ *in the exterior domain* E.

Proof. For sufficiently large R, we may write

$$0 = \int_{E \cap B_{R(0)}} u \Delta u \, dV = \int_{\partial B_R(0)} u \frac{\partial u}{\partial n} ds_{\mathbf{x}} - \sum_{i=1}^{N} \int_{\Gamma_i} u \frac{\partial u}{\partial n} ds_{\mathbf{x}} - \int_{E \cap B_R(0)} |\nabla u|^2 \, dV.$$

Since $u(\mathbf{x})$ takes on some constant value ϕ_i on Γ_i, we may write

$$\int_{E \cap B_R(0)} |\nabla u|^2 \, dV = \int_{\partial B_R(0)} u \frac{\partial u}{\partial n} ds_{\mathbf{x}} - \sum_{i=1}^{N} \phi_i \int_{\Gamma_i} \frac{\partial u}{\partial n} ds_{\mathbf{x}}$$

$$= \int_{\partial B_R(0)} u \frac{\partial u}{\partial n} ds_{\mathbf{x}},$$

since the q_i are all zero. From Lemma 1, the boundedness of u, and the monotone convergence theorem, it is easy to see that

$$\int_E |\nabla u|^2 \, dV = \lim_{R \to \infty} \int_{E \cap B_R(0)} |\nabla u|^2 \, dV = \lim_{R \to \infty} \int_{\partial B_R(0)} u \frac{\partial u}{\partial n} ds_{\mathbf{x}} = 0.$$

Thus, $\nabla u \equiv \mathbf{0}$ in E and u must be a constant. From the decay condition at infinity, $u \equiv 0$ as desired. $\qquad \square$

To develop an integral equation for the elastance problem, we will use the language of scattering theory. That is, we will construct an "incident field" which satisfies the charging conditions (6) but not the boundary conditions (5). We will then solve for a "scattered" field which forces the conductors to be equipotential surfaces without changing the net charge on any of the Γ_i. (This will also yield a proof of existence of solutions.)

Remark 4. *In physical terms, one can think of the problem as follows: imagine that we simply deposit charge uniformly on each conducting surface Γ_i to satisfy the charging condition. This will be our incident field. The charges will then redistribute themselves on each Γ_i so that they are equipotential surfaces. The total field will be defined by that new, equilibrated charge distribution.*

2.1 Mathematical preliminaries

Let γ be a smooth closed curve in $\mathbb{R}^2$ and let $D^{\mp}$ denote the domains corresponding to the interior and exterior of γ. Let $\mathbf{n_x}$ be the unit outward normal to the curve γ and let $\mathbf{n}_0 = \mathbf{n_{x_0}}$ for $\mathbf{x}_0 \in \gamma$. Let $\mu : \gamma \to \mathbb{R}$ be a continuous function. The single layer potential is defined by

$$S_\gamma \mu\left(\mathbf{x}\right) = \int_\gamma G\left(\mathbf{x}, \mathbf{y}\right) \mu\left(\mathbf{y}\right) ds_\mathbf{y}, \tag{9}$$

where $G(\mathbf{x}, \mathbf{y})$ is the fundamental solution for the Laplace equation in free space:

$$G\left(\mathbf{x}, \mathbf{y}\right) = -\frac{1}{2\pi} \log\left|\mathbf{x} - \mathbf{y}\right| . \tag{10}$$

Lemma 3. [20,29,30] *Let $S_\gamma \mu\left(\mathbf{x}\right)$ be a single layer potential with charge density μ defined on γ. Then $S_\gamma \mu\left(\mathbf{x}\right)$ is harmonic in $\mathbb{R}^2 \backslash \gamma$ and continuous in $\mathbb{R}^2$. The single layer potential satisfies the jump relations*

$$\lim_{\substack{\mathbf{x} \to \mathbf{x}_0 \\ \mathbf{x} \in D^\pm}} \frac{\partial S_\gamma \mu\left(\mathbf{x}\right)}{\partial n_{0,\pm}} = \mp\frac{1}{2}\mu\left(\mathbf{x}_0\right) + \oint_\gamma \frac{\partial G\left(\mathbf{x}_0, \mathbf{y}\right)}{\partial n_0} \mu\left(\mathbf{y}\right) ds_\mathbf{y} \tag{11}$$

where $\oint_\gamma$ indicates the principal value integral over the curve γ and the subscripts $-$ and $+$ denote the limits of the integral from the interior and exterior side, respectively. Furthermore,

$$-\int_\gamma \frac{\partial S_\gamma \mu\left(\mathbf{x}\right)}{\partial n_{\mathbf{x},+}} ds_\mathbf{x} = \int_\gamma \mu\left(\mathbf{x}\right) ds_\mathbf{x}, \quad \int_\gamma \frac{\partial S_\gamma \mu\left(\mathbf{x}\right)}{\partial n_{\mathbf{x},-}} ds_\mathbf{x} = 0. \tag{12}$$

For a closed curve $\omega \subset D^+$, we also have

$$\int_\omega \frac{\partial S_\gamma \mu\left(\mathbf{x}\right)}{\partial n_\mathbf{x}} ds_\mathbf{x} = 0. \tag{13}$$

Finally,

$$\left| S_\gamma \mu\left(\mathbf{x}\right) + \frac{1}{2\pi} Q \log\left(\mathbf{x}\right) \right| \to 0 \quad as \ \left|\mathbf{x}\right| \to \infty, \tag{14}$$

where

$$Q = \int_\gamma \mu\left(\mathbf{y}\right) ds_\mathbf{y}.$$

6

The double layer potential $D_\gamma \mu(\mathbf{x})$ is the potential due to a surface density of dipole sources on γ, aligned in the normal direction to the curve:

$$D_\gamma \mu\left(\mathbf{x}\right) = \int_\gamma \frac{\partial G\left(\mathbf{x}, \mathbf{y}\right)}{\partial n_\mathbf{y}} \mu\left(\mathbf{y}\right) ds_\mathbf{y} \tag{15}$$

Lemma 4. *[20, 29, 30] Let $D_\gamma \mu\left(\mathbf{x}\right)$ be a double layer potential. Then, $D_\gamma \mu\left(\mathbf{x}\right)$ is harmonic in $\mathbb{R}^2 \backslash \gamma$ and satisfies the jump relations:*

$$\lim_{\substack{\mathbf{x} \to \mathbf{x}_0 \\ \mathbf{x} \in D^\pm}} D_\gamma \mu = \pm \frac{1}{2} \mu\left(\mathbf{x}_0\right) + \oint_\gamma \frac{\partial G\left(\mathbf{x}_0, \mathbf{y}\right)}{\partial n_\mathbf{y}} \mu\left(\mathbf{y}\right) ds_\mathbf{y} \,. \tag{16}$$

Furthermore,

$$\int_\gamma \frac{\partial G\left(\mathbf{x}, \mathbf{y}\right)}{\partial n_\mathbf{y}} ds_\mathbf{y} = \begin{cases} -1 & \mathbf{x} \in D^- \\ 0 & \mathbf{x} \in D^+ \end{cases} \tag{17}$$

$$\oint_\gamma \frac{\partial G\left(\mathbf{x}, \mathbf{y}\right)}{\partial n_\mathbf{y}} ds_\mathbf{y} = -\frac{1}{2} \quad \mathbf{x} \in \gamma\,, \tag{18}$$

and

$$\left| D_\gamma \mu\left(\mathbf{x}\right) \right| \to 0 \quad as \ \left| \mathbf{x} \right| \to \infty \,. \tag{19}$$

2.2 Charging the boundaries with an incident field

In the elastance problem, perhaps the simplest way to allocate the net charge q_i to the boundary Γ_i is to define a constant charge density

$$\sigma_i(\mathbf{x}) = \frac{q_i}{\left|\Gamma_i\right|}\,, \tag{20}$$

for $\mathbf{x}$ on the curve Γ_i, where $\left|\Gamma_i\right|$ denotes its length. We can then define $\sigma\left(\mathbf{x}\right) = \left(\sigma_1\left(\mathbf{x}\right), \sigma_2\left(\mathbf{x}\right) \ldots \sigma_N\left(\mathbf{x}\right)\right)$ and

$$u_{inc}\left(\mathbf{x}\right) = S_\Gamma \sigma\left(\mathbf{x}\right) \tag{21}$$

where S_Γ is the operator given by

$$S_\Gamma \sigma\left(\mathbf{x}\right) = \sum_{j=1}^N S_{\Gamma_j} \sigma_j\left(\mathbf{x}\right) = \sum_{j=1}^N \int_{\Gamma_j} G\left(\mathbf{x}, \mathbf{y}\right) \sigma_j\left(\mathbf{y}\right) ds_\mathbf{y} \,.$$

From (12) and (13), we have

$$-\int_{\Gamma_j} \frac{\partial u_{inc}\left(\mathbf{x}\right)}{\partial n} ds_\mathbf{x} = \int_{\Gamma_j} \sigma_j\left(\mathbf{x}\right) ds_\mathbf{x} = \frac{q_j}{\left|\Gamma_j\right|} \int_{\Gamma_j} ds_\mathbf{x} = q_j \,, \tag{22}$$

for $j = 1, 2, \ldots, N$. Thus, u_{inc} satisfies the charge constraints (6).

2.3 The scattered field

We now seek a scattered field

$$u_{sc}\left(\mathbf{x}\right) = S_\Gamma \mu\left(\mathbf{x}\right) \tag{23}$$

such that $u(\mathbf{x}) = u_{inc}(\mathbf{x}) + u_{sc}(\mathbf{x})$, where $\mu(\mathbf{x}) = (\mu_1(\mathbf{x}), \mu_2(\mathbf{x}), \ldots, \mu_N(\mathbf{x}))$ with μ_j an unknown charge density on the boundaries Γ_j. To ensure that no additional net charge has been introduced on any of the conductors, we impose the N integral constraints on $\mu\left(\mathbf{x}\right)$:

$$\int_{\Gamma_j} \mu_j\left(\mathbf{x}\right) ds_{\mathbf{x}} = 0\,.$$

If we can find such functions $\mu_j(\mathbf{x})$, then

$$u(\mathbf{x}) = u_{inc}(\mathbf{x}) + u_{sc}(\mathbf{x}) = S_\Gamma(\mu + \sigma)(\mathbf{x})\,, \tag{24}$$

solves the elastance problem. Physically, $(\mu_j + \sigma_j)(\mathbf{x})$ is the final charge density on Γ_j once the total charge place on the boundary has equilibrated to enforce the perfect conductor boundary condition (5).

2.4 Formulation as a Neumann problem

Letting $u(\mathbf{x}) = u_{inc}(\mathbf{x}) + u_{sc}(\mathbf{x})$, note first that the corresponding potential is also defined inside each conductor. Rather than imposing the boundary condition (5) from the exterior, however, we can make use of the fact that the electric field inside each conductor given by $\nabla u\left(\mathbf{x}\right)$ must be identically zero. Thus, we may impose the interior Neumann boundary conditions

$$\frac{\partial u}{\partial n_-}\left(\mathbf{x}\right) \equiv 0 \tag{25}$$

for $\mathbf{x} \in \Gamma$. Using (11), we obtain the following second kind integral equation:

$$\left(\frac{1}{2}I + K\right)\mu\left(\mathbf{x}\right) = -\left(\frac{1}{2}I + K\right)\sigma\left(\mathbf{x}\right) \tag{26}$$

for $\mathbf{x} \in \Gamma$, subject to the constraints

$$\int_{\Gamma_j} \mu_j\left(\mathbf{x}\right) ds_{\mathbf{x}} = 0, \tag{27}$$

for $j = 1, 2, \ldots N$. Here,

$$I = \begin{pmatrix} I_1 & & & \\ & I_2 & & \\ & & \ddots & \\ & & & I_N \end{pmatrix}, \tag{28}$$

$$K = \begin{pmatrix} K_{1,1} & K_{1,2} & \ldots & K_{1,N} \\ K_{2,1} & K_{2,2} & \ldots & K_{2,N} \\ \vdots & \vdots & \ddots & \vdots \\ K_{N,1} & K_{N,2} & & K_{N,N} \end{pmatrix}, \tag{29}$$

$I_i : C^{0,\alpha}(\Gamma_i) \to C^{0,\alpha}(\Gamma_i)$ is the identity map, $K_{i,j} : C^{0,\alpha}(\Gamma_j) \to C^{0,\alpha}(\Gamma_i)$, and $K_{i,i} : C^{0,\alpha}(\Gamma_i) \to C^{0,\alpha}(\Gamma_i)$ are the operators given by

$$K_{i,j}\sigma = \int_{\Gamma_j} \frac{\partial G(\mathbf{x}, \mathbf{y})}{\partial n_{\mathbf{x}}} \sigma(\mathbf{y}) ds_{\mathbf{y}} \quad \mathbf{x} \in \Gamma_i \tag{30}$$

$$K_{i,i}\sigma = \oint_{\Gamma_i} \frac{\partial G(\mathbf{x}, \mathbf{y})}{\partial n_{\mathbf{x}}} \sigma(\mathbf{y}) ds_{\mathbf{y}} \quad \mathbf{x} \in \Gamma_i, \tag{31}$$

where $C^{0,\alpha}(\Gamma)$ is the Hölder space with exponent α and $\alpha > 0$. For a related treatment of the capacitance problem, see [5].

Theorem 1. *Let $u(\mathbf{x})$ be defined as in (24). If $\mu(\mathbf{x})$ solves equations (26) and (27), then $u(\mathbf{x})$ solves the elastance problem.*

Proof. Note first that $u(\mathbf{x})$ is harmonic in E by construction. Using (12) and (13), the choice of σ in equation (20) and the constraints (27), we see that $u(\mathbf{x})$ satisfies the charge constraints (6). Furthermore, from equations (8) and (14), it follows that $u(\mathbf{x}) \to 0$ as $|\mathbf{x}| \to \infty$. Since $u(\mathbf{x})$ is harmonic in D_i and satisfies $\frac{\partial u}{\partial n_-} \equiv 0$ on Γ_i, $u(\mathbf{x}) \equiv c_i$ for some constant c_i inside D_i. By the continuity of the single layer potential, $u = c_i$ from the exterior side of Γ_i as well. $\square$

Remark 5. *(**The adjoint operator**): The operator K in equation (26) is a compact operator for smooth Γ. Hence, $\frac{1}{2}I + K$ is a Fredholm integral equation of the second kind. To study existence of solutions to $\left(\frac{1}{2}I + K\right)\mu = f$, we shall study existence of solutions for the adjoint problem $\left(\frac{1}{2}I + K^*\right)\mu = f$ instead, where*

$$K^* = \begin{pmatrix} K^*_{1,1} & K^*_{1,2} & \ldots & K^*_{1,N} \\ K^*_{2,1} & K^*_{2,2} & \ldots & K^*_{2,N} \\ \vdots & \vdots & \ddots & \vdots \\ K^*_{N,1} & K^*_{N,2} & & K^*_{N,N} \end{pmatrix}. \tag{32}$$

9

Here, $K_{i,j}^* : C^{0,\alpha}(\Gamma_j) \to C^{0,\alpha}(\Gamma_i)$ and $K_{i,i}^* : C^{0,\alpha}(\Gamma_i) \to C^{0,\alpha}(\Gamma_i)$ are the operators given by

$$K_{i,j}^*\sigma = \int_{\Gamma_j} \frac{\partial G(\mathbf{x},\mathbf{y})}{\partial n_\mathbf{y}} \sigma(\mathbf{y})\, ds_\mathbf{y} \tag{33}$$

$$K_{i,i}^*\sigma = \oint_{\Gamma_i} \frac{\partial G(\mathbf{x},\mathbf{y})}{\partial n_\mathbf{y}} \sigma(\mathbf{y})\, ds_\mathbf{y} \tag{34}$$

It is straightforward to verify that $K_{i,j}^*\sigma(\mathbf{x}) = D_{\Gamma_j}\sigma(\mathbf{x})$ for $\mathbf{x} \in \Gamma_i$.

Let $\sigma = \{\sigma_i(\mathbf{x})\}_{i=1}^N$ where each $\sigma_i(\mathbf{x})$, supported on Γ_i, is constant. Then, using (17),(18) and (32), we may conclude that $\left(\frac{1}{2}I + K^*\right)\sigma = 0$. Thus, the dimension of the null space of $\frac{1}{2}I + K^*$ is at least N. In fact, it is well-known that the dimension of the null space is exactly N [20, 29].

Remark 6. $\frac{1}{2}I + K^*$ is the integral operator one would obtain in seeking to impose Dirichlet boundary conditions with the potential represented as a double layer potential. The double layer potential operator for the exterior, however, is range deficient. It cannot represent a harmonic function $u(\mathbf{x})$ in the exterior which is generated by net charge in any of the domains D_i. To see this, note that the net charge is $-\int_{\Gamma_i} \frac{\partial u}{\partial n}$ from (12), but that the double layer potentials satisfies $\int_{\Gamma_i} \frac{\partial u}{\partial n} = 0$ for $i = 1, 2, \ldots N$ from (17).

2.5 Existence of solutions

From the preceding discussion (the existence of a nontrivial nulllspace), it follows from the Fredholm alternative that $\left(\frac{1}{2}I + K\right)\mu = f$ has an N dimensional space of solutions, so long as f is in the range of the operator $\frac{1}{2}I + K$. Using our representation for the elastance problem, the right hand side in equation (26) is certainly in the range of the operator $\frac{1}{2}I + K$. The role of the additional N integral constraints is, therefore, to pick out the unique one which doesn't alter the net charge on the N conductors. However, we do not wish to solve an overdetermined (non-square) linear system. If we simply discretize the integral equation using, say a Nyström method, with M points on Γ, we would have to solve an $(M+N) \times M$ linear system to obtain the desired solution. Instead, we propose to solve the integral equation

$$\frac{1}{2}\mu_i(\mathbf{x}) + \sum_{j=1}^N K_{i,j}\mu_j(\mathbf{x}) + \int_{\Gamma_i} \mu_i(\mathbf{x})ds_\mathbf{x} = -\frac{1}{2}\sigma_i(\mathbf{x}) - \sum_{j=1}^N K_{i,j}\sigma_j(\mathbf{x})$$

for $\mathbf{x} \in \Gamma_i$, or

$$\left(\frac{1}{2}I + K + L\right)\mu = -\left(\frac{1}{2}I + K\right)\sigma \tag{35}$$

where

$$
L = \begin{pmatrix} L_1 & & & \\ & L_2 & & \\ & & \ddots & \\ & & & L_N \end{pmatrix}, \tag{36}
$$

with $L_i : C^{0,\alpha}(\Gamma_i) \to C^{0,\alpha}(\Gamma_i)$ defined by $L_i \mu_i(\mathbf{x}) = \int_{\Gamma_i} \mu_i(\mathbf{y}) ds_{\mathbf{y}}$.

The following lemma shows that solving (35) is equivalent to solving (26) with constraints (27).

Lemma 5. *If μ solves equation (35), then μ solves equations (26) and (27)*

Proof. Using equation (13), we observe that $\int_{\Gamma_i} K_{i,j} \mu_j(\mathbf{x}) ds_{\mathbf{x}} = 0$ for $j \neq i$. Furthermore, switching the order of integration in $\oint_{\Gamma_i} K_{i,i} \mu_i(\mathbf{x}) ds_{\mathbf{x}}$ and using property (18) of the double layer potential, we see that

$$
\oint_{\Gamma_i} K_{i,i} \mu_i(\mathbf{x}) ds_{\mathbf{x}} = \int_{\Gamma_i} \oint_{\Gamma_i} \frac{\partial G(\mathbf{x}, \mathbf{y})}{\partial n_{\mathbf{x}}} \mu_i(\mathbf{y}) ds_{\mathbf{y}} ds_{\mathbf{x}} \tag{37}
$$

$$
= \int_{\Gamma_i} \mu_i(\mathbf{y}) \oint_{\Gamma_i} \frac{\partial G(\mathbf{x}, \mathbf{y})}{\partial n_{\mathbf{x}}} ds_{\mathbf{x}} ds_{\mathbf{y}} \tag{38}
$$

$$
= -\frac{1}{2} \int_{\Gamma_i} \mu_i(\mathbf{y}) ds_{\mathbf{y}}. \tag{39}
$$

Integrating expression (35) on Γ_i, we may conclude that

$$
|\Gamma_i| \int_{\Gamma_i} \mu_i(\mathbf{x}) ds_{\mathbf{x}} = 0. \tag{40}
$$

Thus, $L_i \mu_i(\mathbf{x}) = 0$, which implies that μ satisfies the integral constraints (27) and that

$$
\left(\frac{1}{2} I + K + L \right) \mu = \left(\frac{1}{2} I + K \right) \mu = -\left(\frac{1}{2} I + K \right) \sigma. \tag{41}
$$

$\square$

Remark 7. *For further discussion of the solution of consistent linear systems with constraints in the finite dimensional case, see [31].*

The following lemma shows that the operator $\frac{1}{2} I + K + L$ has no null space.

Lemma 6. *The operator $\frac{1}{2} I + K + L$ is injective.*

Proof. Let $\mu \in \mathcal{N}\left(\frac{1}{2} I + K + L\right)$, i.e. it solves $\left(\frac{1}{2} I + K + L\right) \mu = 0$. Following the proof of Lemma 5, we conclude that $L\mu = 0$ and therefore $\left(\frac{1}{2} I + K\right) \mu = 0$. Let $u = S_\Gamma \mu$. From the properties of the single layer potential

$$
\frac{\partial u}{\partial n_-} = \left(\frac{1}{2} I + K \right) \mu = 0. \tag{42}
$$

11

By uniqueness of solutions to interior Neumann problem, we conclude that u is a constant on each boundary component. Thus, u solves the Elastance problem with $q_i = 0$, as $L\mu = 0$. By uniqueness of solutions to the Elastance problem, we conclude that $u \equiv 0$ in E. Hence, $\frac{\partial u}{\partial n}_+ = 0$. From the properties of the single layer,

$$\mu = \frac{\partial u}{\partial n}_- - \frac{\partial u}{\partial n}_+ = 0 \,. \tag{43}$$

Therefore, $\mathcal{N}\left(\frac{1}{2}I + K + L\right) = \{0\}$. $\qquad\qquad\qquad\qquad\qquad\square$

By the Fredholm alternative, we conclude that (35) has a unique solution μ.

3 The mobility problem

Supose now that we have N rigid bodies immersed in an incompressible Stokesian fluid in $\mathbb{R}^2$. Let $\mathbf{F}_i, T_i$ denote the force and torque exerted on rigid body D_i in a fluid which is otherwise assumed to be at rest and let $\mathbf{v}_i, \omega_i$ be the corresponding rigid body motion, where ω_i is the angular velocity about the centroid of D_i. The mobility matrix $\mathbf{M} \in \mathbb{R}^{3N \times 3N}$ is the linear mapping from the forces and torques on the rigid bodies to the respective rigid body motions:

$$\overline{\mathbf{U}} = \mathbf{M}\overline{\mathbf{F}}$$

where $\overline{\mathbf{U}} = (\mathbf{v}_1, \omega_1, \ldots, \mathbf{v}_N, \omega_N)$ and $\overline{\mathbf{F}} = (\mathbf{F}_1, T_1, \ldots, \mathbf{F}_N, T_N)$.

Referring to Fig. (1), let D_i now represent the rigid bodies and let E represent the Stokesian fluid with viscosity $\mu = 1$. Further, let us assume that there are no other volume forces on the fluid. Let $\mathbf{u}(\mathbf{x}) = (u_1(\mathbf{x}), u_2(\mathbf{x}))$ represent the fluid velocity in E and let $(\mathbf{F}_1, T_1, \ldots, \mathbf{F}_N, T_N)$ be the force and torque exerted on the rigid bodies. Let $\mathbf{x}_i^c = \frac{1}{|\Gamma_i|}\int_{\Gamma_i} \mathbf{x} ds_{\mathbf{x}}$ be the centroid of Γ_i. Let p be the fluid pressure and let $\boldsymbol{\sigma}$ be the stress tensor associated with the flow:

$$\sigma_{ij} = -p\delta_{ij} + \left(\frac{\partial u_i}{\partial x_j} + \frac{\partial u_j}{\partial x_i}\right) = -p\delta_{ij} + 2e\left(\mathbf{u}\right) \tag{44}$$

where δ_{ij} is the Kronecker delta,

$$e\left(\mathbf{u}\right) = \frac{1}{2}\left(D\mathbf{u} + D\mathbf{u}^T\right) \tag{45}$$

is the strain tensor associated with the flow, and $D\mathbf{u}$ is the gradient of $\mathbf{u}$.

On the surface of rigid bodies Γ_i,

$$\mathbf{f} = \boldsymbol{\sigma} \cdot \mathbf{n} = \begin{bmatrix} \sigma_{11} & \sigma_{12} \\ \sigma_{21} & \sigma_{22} \end{bmatrix} \begin{bmatrix} n_1 \\ n_2 \end{bmatrix} \tag{46}$$

represents the surface force or surface traction exerted by the fluid on D_i, where $\mathbf{n}$ is the outward normal to Γ_i. For notational convenience, let $\mathbf{x}^\perp = \begin{bmatrix} -x_2 \\ x_1 \end{bmatrix}$

and $\nabla^{\perp} = \begin{bmatrix} -\frac{\partial}{\partial x_2} \\ \frac{\partial}{\partial x_1} \end{bmatrix}$. Then $\mathbf{u}(\mathbf{x})$ solves [12, 13]

$$-\Delta \mathbf{u} + \nabla p = 0 \quad \text{in E} \tag{47}$$

$$\nabla \cdot \mathbf{u} = 0 \quad \text{in E} \tag{48}$$

$$\mathbf{u}(\mathbf{x})|_{\Gamma_i} = \mathbf{v}_i + \omega_i (\mathbf{x} - \mathbf{x}_i^c)^{\perp} \tag{49}$$

$$\int_{\Gamma_i} \mathbf{f}\, ds_{\mathbf{x}} = \int_{\Gamma_i} \boldsymbol{\sigma}.\mathbf{n}\, ds_{\mathbf{x}} = -\mathbf{F}_i \tag{50}$$

$$\int_{\Gamma_i} (\mathbf{f}, (\mathbf{x} - \mathbf{x}_i^c)^{\perp})\, ds_{\mathbf{x}} = -T_i \tag{51}$$

$$\mathbf{u}(\mathbf{x}) \to \mathbf{0} \quad \text{as } |\mathbf{x}| \to \infty, \tag{52}$$

where $(\mathbf{a}, \mathbf{b})$ represents the Euclidean inner product for vectors $\mathbf{a}, \mathbf{b} \in \mathbb{R}^2$. Equations (47) and (48) are the governing equations for Stokes flow in domain E. Equation (49) enforces a rigid body motion on D_i, where $\mathbf{v}_i, \omega_i$ are unknown. Equations (50) and (51) state the net applied forces and torques are given by the *known* quantities $(\mathbf{F}_i, T_i)$. Finally, (52) states that the fluid is at rest in the absense of forcing. As a consequence of Stokes paradox, there might not exist a solution to the set of equations described above. In fact, it can be shown that

$$\mathbf{u}(\mathbf{x}) = O\left(-\sum_{i=1}^{N} \mathbf{F}_i \log |\mathbf{x}|\right). \tag{53}$$

Thus, a necessary condition for a solution to exist is that

$$\sum_{i=1}^{N} \mathbf{F}_i = 0. \tag{54}$$

From [12, 13], it turns out that (54) is also sufficient for a solution satisyfing equation (52). To prove uniqueness for the mobility problem, we need the following lemmas which can be found in [32].

Lemma 7. *If h is a bounded harmonic function in E and n is an integer greater than 0, with $h = O(r^{-n})$ as $r \to \infty$, then*

$$h(r, \theta) = \sum_{k=n}^{\infty} r^{-k} a_k(\theta), \tag{55}$$

which converges uniformly outside $B_R(0)$ for some R.

Let ω be the vorticity corresponding to the flow, defined by

$$\omega = (\nabla^{\perp}, \mathbf{u}). \tag{56}$$

Lemma 8. *If $\mathbf{u}$ satisfies equation (52), then $\omega = O(r^{-1})$ as $r \to \infty$.*

Lemma 9. *If $\omega = O\left(r^{-n}\right)$ as $r \to \infty$ for integer $n > 0$, then $p = O\left(r^{-n}\right)$ as $r \to \infty$.*

Using these two lemmas, it follows that

Lemma 10. *If $\mathbf{u}$ satisfies equation (52), then on $\partial B_r\left(0\right)$,*

$$p\left(\mathbf{u}, \mathbf{n}\right) - \omega\left(\mathbf{u}^{\perp}, \mathbf{n}\right) = O\left(r^{-1}\right) \quad as \ r \to \infty. \tag{57}$$

Lemma 11. *If $\mathbf{u}$ satisfies equations (49), (50) and (51) with $\mathbf{F}_i = \mathbf{0}$ and $T_i = 0$, then*

$$\int_{\Gamma_i} \left(\mathbf{u}, \mathbf{f}\right) ds_{\mathbf{x}} = 0. \tag{58}$$

Proof.

$$\int_{\Gamma_i} \left(\mathbf{u}, \mathbf{f}\right) ds_{\mathbf{x}} = \int_{\Gamma_i} \left(\mathbf{v}_i + \omega_i \left(\mathbf{x} - \mathbf{x}_i^c\right)^{\perp}, \mathbf{f}\right) ds_{\mathbf{x}} = -\left(\mathbf{v}_i, \mathbf{F}_i\right) - \omega_i T_i = 0. \tag{59}$$

$\square$

Lemma 12. *If $\mathbf{u}$ satisfies equations (49), (50) and (51) with $\mathbf{F}_i = \mathbf{0}$ and $T_i = 0$, then*

$$\int_{\Gamma_i} p\left(\mathbf{u}, \mathbf{n}\right) - \omega\left(\mathbf{u}^{\perp}, \mathbf{n}\right) ds_{\mathbf{x}} = -4\omega_i^2 \left|D_i\right| \tag{60}$$

Proof. On Γ_i, $e\left(\mathbf{u}\right) = 0$ and $\omega = 2\omega_i$. Using Lemma 11 and the divergence theorem

$$-\int_{\Gamma_i} \left(\mathbf{u}, \mathbf{f}\right) + 2\omega_i \left(\mathbf{v}_i^{\perp} + \omega_i \left(\mathbf{x} - \mathbf{x}_i^c\right), \mathbf{n}\right) ds_{\mathbf{x}} = -4\omega_i^2 \left|D_i\right| \tag{61}$$

$\square$

Lemma 13 (adapted from [32]). *If $\mathbf{u}\left(\mathbf{x}\right)$ satisifies equations (47), (48), (49), (50), (51) and (52) with $\mathbf{F}_i = \mathbf{0}$ and $T_i = 0$, then*

$$\lim_{R \to \infty} \int_{\partial B_R\left(0\right)} \left(\mathbf{u}, \mathbf{f}\right) ds_{\mathbf{x}} \to 0. \tag{62}$$

Proof. For large enough R, Lemma 12 yields

$$\int_{E \cap B_R\left(0\right)} \omega^2 dV = \sum_{i=1}^{N} \int_{\Gamma_i} p\left(\mathbf{u}, \mathbf{n}\right) - \omega\left(\mathbf{u}^{\perp}, \mathbf{n}\right) ds_{\mathbf{x}}$$

$$- \int_{\partial B_R\left(0\right)} p\left(\mathbf{u}, \mathbf{n}\right) - \omega\left(\mathbf{u}^{\perp}, \mathbf{n}\right) ds_{\mathbf{x}} \tag{63}$$

$$= -4\sum_{i=1}^{N} \omega_i^2 \left|D_i\right| - \int_{\partial B_R\left(0\right)} p\left(\mathbf{u}, \mathbf{n}\right) - \omega\left(\mathbf{u}^{\perp}, \mathbf{n}\right) ds_{\mathbf{x}}. \tag{64}$$

14

Using Lemma 10, we conclude that

$$\int_E \omega^2 dV < \infty \, . \tag{65}$$

Using Lemma 7, we know that

$$\omega(r,\theta) = r^{-1} a_1(\theta) + O\left(r^{-2}\right) \, . \tag{66}$$

Integrating ω^2 in the annulus $B = B_r(0) \cap B_{\bar{R}}(0)^C$, we get

$$\int_B \omega^2 dV = \log\left(\frac{r}{\bar{R}}\right) \int_0^{2\pi} a_1^2(\theta)d\theta + O\left(r^{-2}\right) \, . \tag{67}$$

Since $\int_B \omega^2 dV$ is bounded, we conclude that $a_1 \equiv 0$ and that $\omega = O\left(r^{-2}\right)$. Using Lemma 9, we conclude that $p = O\left(r^{-2}\right)$. Thus

$$\int_{\partial B_R(0)} \left[-p\left(\mathbf{u},\mathbf{n}\right) + \omega\left(\mathbf{u}^\perp,\mathbf{n}\right) \right] ds_{\mathbf{x}} \to 0 \quad \text{as} \quad R \to \infty \, . \tag{68}$$

From equation (64), it follows that $\omega \equiv 0$ in E. Using equation (48), we conclude that $\Delta \mathbf{u} = 0$ in E. Using the estimate for p and Lemma 1, we get $\mathbf{f} = O\left(r^{-2}\right)$. Using this estimate and the decay condition in $\mathbf{u}$ at ∞, the result follows. $\qquad \square$

The following lemma is a modification of the standard proof of uniqueness for Stokes flow [12, 13].

Lemma 14. *If* $\mathbf{u}\left(\mathbf{x}\right)$ *satisifies equations* (47), (48), (49), (50), (51) *and* (52) *with* $\mathbf{F}_i = 0$ *and* $T_i = 0$, *then* $\mathbf{u}\left(\mathbf{x}\right) \equiv 0$.

Proof. Let $\langle \cdot, \cdot \rangle : \mathbb{R}^{2\times 2} \times \mathbb{R}^{2\times 2}$ be the Frobenius inner product. For large enough R,

$$\int_{E\cap B_R(0)} \langle e\left(\mathbf{u}\right), e\left(\mathbf{u}\right) \rangle dV = \int_{E\cap B_R(0)} \langle D\mathbf{u}, e\left(\mathbf{u}\right) \rangle dV$$

$$= \int_{\partial(E\cap B_R(0))} \left(\mathbf{u}, e\left(\mathbf{u}\right) \cdot \mathbf{n}\right) ds_{\mathbf{x}} - \frac{1}{2} \int_{E\cap B_R(0)} \left(\mathbf{u}, \Delta\mathbf{u}\right) dV$$

$$= \int_{\partial(E\cap B_R(0))} \left(\mathbf{u}, e\left(\mathbf{u}\right) \cdot \mathbf{n}\right) ds_{\mathbf{x}} - \frac{1}{2} \int_{E\cap B_R(0)} \left(\mathbf{u}, \nabla p\right) dV$$

$$= \frac{1}{2} \int_{\partial(E\cap B_R(0))} \left(\mathbf{u}, \left(-p \begin{bmatrix} 1 & 0 \\ 0 & 1 \end{bmatrix} + 2e\left(\mathbf{u}\right)\right).\mathbf{n}\right) ds_{\mathbf{x}}$$

$$= -\frac{1}{2} \sum_{i=1}^N \int_{\Gamma_i} \left(\mathbf{u}, \mathbf{f}\right) ds_{\mathbf{x}} + \frac{1}{2} \int_{\partial B_R(0)} \left(\mathbf{u}, \mathbf{f}\right) ds_{\mathbf{x}}$$

$$= \frac{1}{2} \int_{\partial B_R(0)} \left(\mathbf{u}, \mathbf{f}\right) ds_{\mathbf{x}} \, .$$

using (48) and Lemma 11. Taking the limit as $R \to \infty$ in the above expression and using equation (62), we get

$$e(\mathbf{u}) \equiv \begin{bmatrix} 0 & 0 \\ 0 & 0 \end{bmatrix} \quad \mathbf{x} \in E. \tag{69}$$

Thus, $\mathbf{u}$ is a rigid body motion. However since $\mathbf{u}(\mathbf{x}) \to \mathbf{0}$ as $|\mathbf{x}| \to \infty$, we conclude that $\mathbf{u} \equiv \mathbf{0}$. $\qquad\square$

We construct an integral representation for the mobility problem by direct analogy with the elastance problem, with the velocity $\mathbf{u}(\mathbf{x})$ playing the role of the potential and surface traction $\mathbf{f}$ playing the role of charge in the elastance problem. (A rigid body has no interior strain or stress, with all the stress residing on the surface.) We first construct an "incident" field which satisfies the net force and torque conditions on each rigid body but which does not correspond to a rigid body motion. We then find a "scattered" velocity induced by an additional force vector μ so that the total velocity will satisfy (49) but does not change the net force and torque. As in the elastance problem, this can be thought of as a redistribution of the surface force.

3.1 Mathematical preliminaries

In the remainder of this paper, we will use the Einstein summation convention. As above, we let γ be a smooth closed curve in $\mathbb{R}^2$ and we let $D^{\mp}$ denote the domains corresponding to the interior and exterior of γ. $\mathbf{n_x} = (n_{\mathbf{x},1}, n_{\mathbf{x},2})$ will be used to denoted the unit outward normal at $\mathbf{x} \in \gamma$ and $\mathbf{n}_0 = (n_{0,1}, n_{0,2})$ to denote the unit outward normal at $\mathbf{x}_0 \in \gamma$. We let $\boldsymbol{\mu}(\mathbf{x}) = (\mu_1(\mathbf{x}), \mu_2(\mathbf{x})) : \gamma \to \mathbb{R}^2$ be a continuous function.

Following the treatment of [12, 13], the fundamental solution to the Stokes equations (the Stokeslet) in free space is given by

$$G_{i,j}(\mathbf{x}, \mathbf{y}) = \frac{1}{4\pi} \left[-\log |\mathbf{x} - \mathbf{y}| \, \delta_{ij} + \frac{(x_i - y_i)(x_j - y_j)}{|\mathbf{x} - \mathbf{y}|^2} \right] \quad i, j \in 1, 2. \tag{70}$$

The Stokeslet allows us to express the velocity field $\mathbf{u} = (u_1, u_2)$ induced by a point force $\mathbf{f} = (f_1, f_2)$ in the form

$$u_i = G_{i,j}(\mathbf{x}, \mathbf{y}) f_j. \tag{71}$$

The single layer Stokes potential is the velocity induced by a surface force on a boundary γ:

$$\mathcal{S}_\gamma \boldsymbol{\mu}(\mathbf{x})_i = \int_\gamma G_{i,j}(\mathbf{x}, \mathbf{y}) \mu_j(\mathbf{y}) \, ds_{\mathbf{y}} \quad \text{for } i = 1, 2. \tag{72}$$

Lemma 15. *Let $\mathcal{S}_\gamma \boldsymbol{\mu}(\mathbf{x})$ denote a single layer Stokes potential of the form (72). Then, $\mathcal{S}_\gamma \boldsymbol{\mu}(\mathbf{x})$ satisfies the Stokes equations in $\mathbb{R}^2 \backslash \gamma$ and $\mathcal{S}_\gamma \boldsymbol{\mu}(\mathbf{x})$ is continuous*

in $\mathbb{R}^2$. Moreover, if we let $\mathbf{f}(\mathbf{x}_0)$ denote the surface traction on γ corresponding to the velocity field $\mathcal{S}_\gamma \boldsymbol{\mu}(\mathbf{x})$, then

$$\lim_{\substack{\mathbf{x} \to \mathbf{x}_0 \\ \mathbf{x} \in D^\pm}} f_{i,\pm}(\mathbf{x}_0) = \mp \frac{1}{2} \mu_i(\mathbf{x}_0) + n_{0,k} \oint_\gamma \mathbf{T}_{i,j,k}(\mathbf{x}_0, \mathbf{y}) \mu_j(\mathbf{y}) \, ds_\mathbf{y} \tag{73}$$

where $\mathbf{T}_{i,j,k}(\mathbf{x}, \mathbf{y})$ is the stresslet corresponding to the flow given by

$$\mathbf{T}_{i,j,k}(\mathbf{x}, \mathbf{y}) = -\frac{1}{\pi} \frac{(x_i - y_i)(x_j - y_j)(x_k - y_k)}{|\mathbf{x} - \mathbf{y}|^4}. \tag{74}$$

The notation $\oint_\gamma$ is used, as above, to denote the principal value integral. The net force and torque on the domain are given by

$$\int_\gamma \mathbf{f}_+ ds_\mathbf{x} = -\int_\gamma \boldsymbol{\mu}(\mathbf{x}) \, ds_\mathbf{x}, \quad \int_\gamma \mathbf{f}_- \, ds_\mathbf{x} = \mathbf{0} \tag{75}$$

and

$$\int_\gamma \left((\mathbf{x} - \mathbf{x}^c)^\perp, \mathbf{f}\right)_+ ds_\mathbf{x} = -\int_\gamma \left((\mathbf{x} - \mathbf{x}^c)^\perp, \boldsymbol{\mu}\right) ds_\mathbf{x}, \tag{76}$$

$$\int_\gamma \left((\mathbf{x} - \mathbf{x}^c)^\perp, \mathbf{f}\right)_- ds_\mathbf{x} = 0. \tag{77}$$

If ω is a closed curve in D^+, then

$$\int_\omega \mathbf{f} \, ds_\mathbf{x} = \mathbf{0} \tag{78}$$

$$\int_\omega \left((\mathbf{x} - \mathbf{x}^c)^\perp, \mathbf{f}\right) ds_\mathbf{x} = 0. \tag{79}$$

Finally,

$$\left| \mathcal{S}_\gamma \boldsymbol{\mu}(\mathbf{x}) + \frac{1}{4\pi} \left[\log(\mathbf{x}) \begin{bmatrix} 1 & 0 \\ 0 & 1 \end{bmatrix} - \frac{\mathbf{R}}{|x|^2} \right] \int_\gamma \boldsymbol{\mu}(\mathbf{y}) \, ds_\mathbf{y} \right| \to 0 \tag{80}$$

as $|\mathbf{x}| \to \infty$, where

$$\mathbf{R} = \begin{bmatrix} x_1^2 & x_1 x_2 \\ x_1 x_2 & x_2^2 \end{bmatrix}. \tag{81}$$

The double layer Stokes potential is the velocity field due to a surface density of stresslets on the curve:

$$\mathcal{D}_\gamma \boldsymbol{\mu}(\mathbf{x})_i = \int_\gamma \mathbf{T}_{j,i,k}(\mathbf{y}, \mathbf{x}) \mu_j(\mathbf{y}) n_{\mathbf{y},k} \, ds_\mathbf{y}. \tag{82}$$

Lemma 16. *Let $\mathcal{D}_\gamma \boldsymbol{\mu}(\mathbf{x})$ denote a double layer Stokes potential of the form (82). Then, $\mathcal{D}_\gamma \boldsymbol{\mu}(\mathbf{x})$ satisfies the Stokes equation in $\mathbb{R}^2 \backslash \gamma$ and the jump relations:*

$$\lim_{\substack{\mathbf{x} \to \mathbf{x}_0 \\ \mathbf{x} \in D^\pm}} \mathcal{D}_\gamma \mu_i = \pm \frac{1}{2} \mu_i(\mathbf{x}_0) + \oint_\gamma \mathbf{T}_{j,i,k}(\mathbf{y}, \mathbf{x}_0) \mu_j(\mathbf{y}) n_{\mathbf{y},k} \, ds_\mathbf{y}. \tag{83}$$

17

Furthermore,

$$\int_{\gamma} \mathbf{T}_{i,j,k}\left(\mathbf{y},\mathbf{x}\right) n_{\mathbf{y},k}\, ds_{\mathbf{y}} = \begin{cases} -\delta_{ij} & \mathbf{x} \in D \\ 0 & \mathbf{x} \in E \end{cases}, \tag{84}$$

$$\oint_{\gamma} \mathbf{T}_{i,j,k}\left(\mathbf{y},\mathbf{x}\right) n_{\mathbf{y},k}\, ds_{\mathbf{y}} = -\frac{\delta_{ij}}{2} \quad \mathbf{x} \in \gamma. \tag{85}$$

Letting ϵ_{ilj} be the standard Levi-Civita symbol,

$$\int_{\gamma} \epsilon_{ilm} y_l \mathbf{T}_{m,j,k}\left(\mathbf{y},\mathbf{x}\right) n_{\mathbf{y},k}\, ds_{\mathbf{y}} = \begin{cases} -\epsilon_{ilj} x_l & \mathbf{x} \in D \\ 0 & \mathbf{x} \in E \end{cases}, \tag{86}$$

$$\oint_{\gamma} \epsilon_{ilm} y_l \mathbf{T}_{m,j,k}\left(\mathbf{y},\mathbf{x}\right) n_{\mathbf{y},k}\, ds_{\mathbf{y}} = -\frac{\epsilon_{ilj} x_l}{2} \quad \mathbf{x} \in \gamma. \tag{87}$$

Finally,

$$|\mathcal{D}_{\gamma} \boldsymbol{\mu}\left(\mathbf{x}\right)| \to 0 \quad as \ |\mathbf{x}| \to \infty. \tag{88}$$

3.2   Applying the net force and torque as an incident field

We construct a velocity field $\mathbf{u}_{inc}\left(\mathbf{x}\right)$ in the exterior domain E, due to set of surface force densities $\left\{\boldsymbol{\rho}_j\left(\mathbf{x}\right)\right\}_{j=1}^{N}$ on the boundaries $\left\{\Gamma_j\right\}_{j=1}^{N}$, which satisfies the force and torque constraints (50) and (51). Each $\boldsymbol{\rho}_j$ is a vector density $\boldsymbol{\rho}_j = (\rho_{1,j}, \rho_{2,j})$. Letting $\boldsymbol{\rho}\left(\mathbf{x}\right) = (\rho_{1,1}\left(\mathbf{x}\right), \rho_{2,1}\left(\mathbf{x}\right) \ldots \rho_{1,N}\left(\mathbf{x}\right), \rho_{2,N}\left(\mathbf{x}\right))$, we define

$$\mathbf{u}_{inc}\left(\mathbf{x}\right) = \mathcal{S}_{\Gamma} \boldsymbol{\rho}\left(\mathbf{x}\right), \tag{89}$$

where $\mathcal{S}_{\Gamma}$ is the operator given by

$$\mathcal{S}_{\Gamma} \boldsymbol{\rho}\left(\mathbf{x}\right)_i = \sum_{j=1}^{N} \mathcal{S}_{\Gamma_j} \boldsymbol{\rho}_j\left(\mathbf{x}\right)_i = \sum_{j=1}^{N} \int_{\Gamma_j} G_{i,k}\left(\mathbf{x},\mathbf{y}\right) \rho_{k,j}\left(\mathbf{y}\right) ds_{\mathbf{y}} \quad i=1,2. \tag{90}$$

If we now let $\mathbf{f}_j$ denote the surface force on Γ_j corresponding to the velocity field $\mathbf{u}_{inc}$ and make use of equations (75) and (78), we obtain

$$\mathbf{F}_j = -\int_{\Gamma_j} \mathbf{f}_j\, ds_{\mathbf{x}} = \int_{\Gamma_j} \boldsymbol{\rho}_j\left(\mathbf{x}\right) ds_{\mathbf{x}} \quad \text{for } j=1,2,\ldots N. \tag{91}$$

Using equations (76), and (79), we obtain

$$T_j = -\int_{\Gamma_j} \left(\left(\mathbf{x} - \mathbf{x}_j^c\right)^{\perp}, \mathbf{f}_j\right) ds_{\mathbf{x}} = \int_{\Gamma_j} \left(\left(\mathbf{x} - \mathbf{x}_j^c\right)^{\perp}, \boldsymbol{\rho}_j\right) ds_{\mathbf{x}}. \tag{92}$$

18

Thus, any choice of $\boldsymbol{\rho}_j(\mathbf{x})$ which satisfies equations (91) and (92) will define an incident field that enforces the desired force and torque conditions. We will use the simple formula

$$\boldsymbol{\rho}_j(\mathbf{x}) = \frac{\mathbf{F}_j}{|\Gamma_j|} + T_j \frac{(\mathbf{x} - \mathbf{x}_j^c)^{\perp}}{W_j}, \tag{93}$$

where $|\Gamma_j|$ is the length of Γ_j and $W_j = \int_{\Gamma_j} |\mathbf{x} - \mathbf{x}_j^c|^2 \, ds_{\mathbf{x}}$.

3.3 The scattered field

We now seek a "scattered" velocity field $\mathbf{u}_{sc}(\mathbf{x})$ induced by unknown surface force densities $\{\boldsymbol{\mu}_j(\mathbf{x})\}_{j=1}^n$ on the boundaries $\{\Gamma_j\}_{j=1}^n$. Each $\boldsymbol{\mu}_j$ is a vector density $\boldsymbol{\mu}_j = (\mu_{1,j}, \mu_{2,j})$. These densities correspond to a redistribution of surface forces that will be used to enforce the rigid body boundary conditions without affecting the net force and torque. We let

$$\boldsymbol{\mu}(\mathbf{x}) = (\mu_{1,1}(\mathbf{x}), \mu_{2,1}(\mathbf{x}) \ldots \mu_{1,N}(\mathbf{x}), \mu_{2,N}(\mathbf{x}))$$

and define

$$\mathbf{u}_{sc}(\mathbf{x}) = \mathcal{S}_{\Gamma} \boldsymbol{\mu}(\mathbf{x}). \tag{94}$$

To ensure that no additional net forces or torques are introduced on the surfaces Γ_i, we need to impose $3N$ integral constraints on $\boldsymbol{\mu}(\mathbf{x})$, namely

$$\int_{\Gamma_j} \mu_{i,j}(\mathbf{x}) \, ds_{\mathbf{x}} = 0, \tag{95}$$

$$\int_{\Gamma_j} \left((\mathbf{x} - \mathbf{x}_j^c)^{\perp}, \boldsymbol{\mu}_j \right) ds_{\mathbf{x}} = 0. \tag{96}$$

The total velocity field is given by

$$\mathbf{u}(\mathbf{x}) = \mathbf{u}_{inc}(\mathbf{x}) + \mathbf{u}_{sc}(\mathbf{x}) = \mathcal{S}_{\Gamma}(\boldsymbol{\mu}(\mathbf{x}) + \boldsymbol{\rho}(\mathbf{x})). \tag{97}$$

3.4 Reformulation as an interior boundary value problem

The function $\mathbf{u}(\mathbf{x}) = \mathcal{S}_{\Gamma}(\boldsymbol{\mu}(\mathbf{x}) + \boldsymbol{\rho}(\mathbf{x}))$ also represents the velocity field inside the rigid bodies. Since there is no internal stress in a rigid body, the stress tensor $\boldsymbol{\sigma}$ must be identically zero within D_i. Thus we will seek to impose

$$\mathbf{f}_- = (\boldsymbol{\sigma} \cdot \mathbf{n})_- \equiv 0 \tag{98}$$

for $\mathbf{x} \in \Gamma$. Using equation (73), we obtain the following Fredholm integral equation of the second kind:

$$\left(\frac{1}{2} \mathbf{I} + \mathcal{K} \right) \boldsymbol{\mu}(\mathbf{x}) = -\left(\frac{1}{2} \mathbf{I} + \mathcal{K} \right) \boldsymbol{\rho}(\mathbf{x}) \quad \mathbf{x} \in \Gamma \tag{99}$$

19

which we subject to the constraints

$$\int_{\Gamma_j} \mu_{i,j}(\mathbf{x}) \, ds_{\mathbf{x}} = 0 \,, \tag{100}$$

$$\int_{\Gamma_j} \left((\mathbf{x} - \mathbf{x}_j^c)^{\perp}, \boldsymbol{\mu}_j\right) ds_{\mathbf{x}} = 0 \,, \tag{101}$$

where

$$\mathbf{I} = \begin{pmatrix} \mathbf{I}_1 & & & \\ & \mathbf{I}_2 & & \\ & & \ddots & \\ & & & \mathbf{I}_N \end{pmatrix}$$

and

$$\mathcal{K} = \begin{pmatrix} \mathcal{K}_{1,1} & \mathcal{K}_{1,2} & \dots & \mathcal{K}_{1,N} \\ \mathcal{K}_{2,1} & \mathcal{K}_{2,2} & \dots & K_{2,N} \\ \vdots & \vdots & \ddots & \vdots \\ \mathcal{K}_{N,1} & \mathcal{K}_{N,2} & & \mathcal{K}_{N,N} \end{pmatrix}.$$

Here, $\mathbf{I}_i : C^{0,\alpha}(\Gamma_i) \times C^{0,\alpha}(\Gamma_i) \to C^{0,\alpha}(\Gamma_i) \times C^{0,\alpha}(\Gamma_i)$ is the identity map, and $\mathcal{K}_{i,j} : C^{0,\alpha}(\Gamma_j) \times C^{0,\alpha}(\Gamma_j) \to C^{0,\alpha}(\Gamma_i) \times C^{0,\alpha}(\Gamma_i)$ is the operator given by

$$(\mathcal{K}_{i,j}\boldsymbol{\rho})_k = n_{\mathbf{x},l} \int_{\Gamma_j} \mathbf{T}_{k,m,l}(\mathbf{x}, \mathbf{y}) \rho_m(\mathbf{y}) \, ds_{\mathbf{y}} \quad \mathbf{x} \in \Gamma_i$$

for $i \neq j$ and

$$(\mathcal{K}_{i,i}\boldsymbol{\rho})_k = n_{\mathbf{x},l} \oint_{\Gamma_i} \mathbf{T}_{k,m,l}(\mathbf{x}, \mathbf{y}) \rho_m(\mathbf{y}) \, ds_{\mathbf{y}} \quad \mathbf{x} \in \Gamma_i \,.$$

Theorem 2. *Let* $\mathbf{u}(\mathbf{x})$ *be the total velocity, defined in* (97). *If* $\boldsymbol{\mu}(\mathbf{x})$ *solves equation* (99), *together with the constraints* (100) *and* (101), *then* $\mathbf{u}(\mathbf{x})$ *solves the mobility problem.*

Proof. $\mathbf{u}(\mathbf{x})$ clearly satisfies the Stokes equations in E by construction. Using equations (75), (76), (78) and (79), the choice of $\boldsymbol{\rho}$ in equation (93), and the constraints (100) and (101), we see that $\mathbf{u}(\mathbf{x})$ satisfies the net force and torque conditions (50) and (51). Furthermore, from (54) and (80), it follows that $|\mathbf{u}(\mathbf{x})| \to 0$ as $|\mathbf{x}| \to \infty$. Since $\mathbf{u}(\mathbf{x})$ solves the Stokes equations in D_i and satisfies $\mathbf{f}_- \equiv 0$ on Γ_i, $\mathbf{u}$ must be a rigid body motion. By the continuity of the single layer potential, $\mathbf{u}$ must define a rigid body motion from the exterior as well. $\qquad\square$

3.5 Existence of solutions

It is well-known that $\frac{1}{2}\mathbf{I} + \mathcal{K}$ has a $3N$-dimensional null space [13]. It follows from the Fredholm alternative that $\left(\frac{1}{2}\mathbf{I} + \mathcal{K}\right)\mu = g$ has an $3N$ dimensional space of solutions, so long as g is in the range of the operator $\frac{1}{2}\mathbf{I} + \mathcal{K}$. From (99), this

is clearly the case, and the purpose of the $3N$ integral constraints is to select the particular solution that doesn't alter the net forces and torques. As for the elastance problem, however, we do not wish to solve a rectangular linear system. If we discretize the integral equation using Nyström quadrature, with M points on Γ, we would have to solve a $(2M + 3N) \times 2M$ linear system to obtain the desired solution. Instead, we propose to solve the integral equation

$$\frac{1}{2}\boldsymbol{\mu}_i(\mathbf{x}) + \sum_{j=1}^{N} \mathcal{K}_{i,j}\boldsymbol{\mu}_j(\mathbf{x}) + \int_{\Gamma_i} \boldsymbol{\mu}_i(\mathbf{y}) \, ds_\mathbf{y}$$

$$+ (\mathbf{x} - \mathbf{x}_c)^\perp \int_{\Gamma_i} \left((\mathbf{y} - \mathbf{x}_i^c)^\perp, \boldsymbol{\mu}_i(\mathbf{y}) \right) ds_\mathbf{y}$$

$$= -\frac{1}{2}\boldsymbol{\rho}_i(\mathbf{x}) - \sum_{j=1}^{N} \mathcal{K}_{i,j}\boldsymbol{\rho}_j(\mathbf{x}) \quad \mathbf{x} \in \Gamma_i \qquad (102)$$

or

$$\left(\frac{1}{2}\mathbf{I} + \mathcal{K} + \mathbf{L}\right)\boldsymbol{\mu} = -\left(\frac{1}{2}\mathbf{I} + \mathcal{K}\right)\boldsymbol{\rho}, \qquad (103)$$

where

$$\mathbf{L} = \begin{pmatrix} \mathbf{L}_1 & & & \\ & \mathbf{L}_2 & & \\ & & \ddots & \\ & & & \mathbf{L}_N \end{pmatrix} \qquad (104)$$

with $\mathbf{L}_i$ defined by

$$\mathbf{L}_i\boldsymbol{\mu}_i(\mathbf{x}) = \int_{\Gamma_i} \boldsymbol{\mu}_i(\mathbf{y}) \, ds_\mathbf{y} + (\mathbf{x} - \mathbf{x}_i^c)^\perp \int_{\Gamma_i} \left((\mathbf{y} - \mathbf{x}_i^c)^\perp, \boldsymbol{\mu}_i(\mathbf{y}) \right) ds_\mathbf{y}. \qquad (105)$$

The following lemma shows that solving (103) is equivalent to solving (99) with the constraints (100) and (101).

Lemma 17. *If $\boldsymbol{\mu}$ solves* (103), *then it solves* (99), (100) *and* (101) .

Proof. Using equation (86), we see that $\int_{\Gamma_i} \left((\mathbf{x} - \mathbf{x}_i^c)^\perp, \mathcal{K}_{i,j}\boldsymbol{\mu}_j(\mathbf{x}) \right) ds_\mathbf{x} = 0$. Similarly, using equation (87), we see that

$$\int_{\Gamma_i} \left((\mathbf{x} - \mathbf{x}_i^c)^\perp, \mathcal{K}_{i,i}\boldsymbol{\mu}_i(\mathbf{x}) \right) ds_\mathbf{x} = -\frac{1}{2}\int_{\Gamma_i} \left((\mathbf{x} - \mathbf{x}_i^c)^\perp, \boldsymbol{\mu}_i(\mathbf{x}) \right) ds_\mathbf{x}. \qquad (106)$$

Since $\mathbf{x}_i^c$ is the centroid of Γ_i, $\int_{\Gamma_i} (\mathbf{x} - \mathbf{x}_i^c)^\perp ds_\mathbf{x} = 0$. Taking the inner product of (103) with $(\mathbf{x} - \mathbf{x}_i^c)^\perp$, integrating the expression over Γ_i, and using the equations above, we obtain

$$\left(\int_{\Gamma_i} |\mathbf{x} - \mathbf{x}_i^c|^2 \, ds_\mathbf{x}\right) \int_{\Gamma_i} \left((\mathbf{y} - \mathbf{x}_i^c)^\perp, \boldsymbol{\mu}_i(\mathbf{y}) \right) ds_\mathbf{y} = 0. \qquad (107)$$

From (84), we observe that $\int_{\Gamma_i} \mathcal{K}_{i,j}\boldsymbol{\mu}_j(\mathbf{x}) \, ds_\mathbf{x} = 0$ for $j \neq i$. Furthermore, switching the order of integration in $\int_{\Gamma_i} \mathcal{K}_{i,i}\boldsymbol{\mu}_i(\mathbf{x}) \, ds_\mathbf{x}$ and using property (85) of the double layer potential, we find that

$$\int_{\Gamma_i} \mathcal{K}_{i,i}\boldsymbol{\mu}_i(\mathbf{x}) \, ds_\mathbf{x} = -\frac{1}{2}\int_{\Gamma_i} \boldsymbol{\mu}_i(\mathbf{x}) \, ds_\mathbf{x} \,. \tag{108}$$

Integrating the expression (103) on Γ_i and using the fact that

$$\int_{\Gamma_i} \left((\mathbf{y} - \mathbf{x}_i^c)^\perp , \boldsymbol{\mu}_i(\mathbf{y}) \right) ds_\mathbf{y} = 0,$$

we may conclude that

$$|\Gamma_i| \int_{\Gamma_i} \boldsymbol{\mu}_i(\mathbf{x}) \, ds_\mathbf{x} = 0 \,. \tag{109}$$

Thus, $\boldsymbol{\mu}$ satisfies the integral constraints (100) and (101), implying that $\mathbf{L}_i\boldsymbol{\mu}_i(\mathbf{x}) = 0$ and that

$$\left(\frac{1}{2}\mathbf{I} + \mathcal{K} + \mathbf{L}\right)\boldsymbol{\mu} = \left(\frac{1}{2}\mathbf{I} + \mathcal{K}\right)\boldsymbol{\mu} = -\left(\frac{1}{2}\mathbf{I} + \mathcal{K}\right)\boldsymbol{\rho} \,. \tag{110}$$

$\square$

The following lemma shows that the operator $\frac{1}{2}\mathbf{I} + \mathcal{K} + \mathbf{L}$ has no null space.

Lemma 18. *The operator $\frac{1}{2}\mathbf{I} + \mathcal{K} + \mathbf{L}$ is injective.*

Proof. Let $\boldsymbol{\mu} \in \mathcal{N}\left(\frac{1}{2}\mathbf{I} + \mathcal{K} + \mathbf{L}\right)$, i.e. it solves $\left(\frac{1}{2}\mathbf{I} + \mathcal{K} + \mathbf{L}\right)\boldsymbol{\mu} = 0$. Following the proof of Lemma 17, we conclude that $\boldsymbol{\mu}$ satisfies the force and torque constraints given by equations (100) and (101). Thus $\mathbf{L}\boldsymbol{\mu} = 0$ and $\left(\frac{1}{2}\mathbf{I} + \mathcal{K}\right)\boldsymbol{\mu} = 0$. Let $\mathbf{u} = \mathcal{S}_\Gamma\boldsymbol{\mu}$. Let $\mathbf{f}_-$ and $\mathbf{f}_+$ denote the interior and exterior limits of the surface traction corresponding to the velocity field $\mathbf{u}$, respectively. From the properties of the Stokes single layer potential

$$\mathbf{f}_- = \left(\frac{1}{2}\mathbf{I} + \mathcal{K}\right)\boldsymbol{\mu} = 0 \,. \tag{111}$$

By uniqueness of solutions to interior surface traction problem, we conclude that $\mathbf{u}$ is a rigid body motion on each boundary component. Thus, $\mathbf{u}$ solves the mobility problem with $\mathbf{F}_i = \mathbf{0}$ and $T_i = 0$. By uniqueness of solutions to the mobility problem, we conclude that $\mathbf{u} \equiv 0$ in E. Hence, $\mathbf{f}_+ = 0$. From the properties of the Stokes single layer,

$$\boldsymbol{\mu} = \mathbf{f}_- - \mathbf{f}_+ = \mathbf{0} \,. \tag{112}$$

Therefore, $\mathcal{N}\left(\frac{1}{2}\mathbf{I} + \mathcal{K} + \mathbf{L}\right) = \{0\}$. $\square$

By the Fredholm alternative, therefore, (103) has a unique solution μ.

4 Numerical Examples

The fact that the capacitance and elastance problems are inverses of each other, and that completely different techniques can be used for their solution, permits a robust test of the performance of our method in arbitrary geometry (without an exact reference solution). The same is true for the resistance and mobility problems.

4.1 The elastance problem

Suppose now that we solve the capacitance problem discussed in section 2 using known techniques (see, [20], for example). That is, given prescribed potentials ϕ_j on a collection of perfect conductors with boundaries Γ_j, we may obtain the charges induced on each conductor. We can then solve the elastance problem with these charges as input, using the representation in section 2, and verify that the corresponding potentials are those used in the original capacitance problem setup. We emphasize that the integral equations used for the capacitance and elastance problems are not inverses of each other, so this provides a nontrivial test of accuracy.

More precisely, following the discussion in section 2, we consider the domain exterior to N perfect conductors D_i whose boundaries are given by Γ_i. We prescribe potentials ϕ_i on the boundaries Γ_i and solve the capacitance problem to obtain the net charge q_i on Γ_i and also the potential at ∞, $u_\infty = \lim_{|\mathbf{x}| \to \infty} u(\mathbf{x})$.

We use these charges as input for the elastance problem and to compute the potentials induced on the conductors, letting $\sigma_{i,el}$ denote the uniformly distributed charge defined in terms of q_i, as in section 2.2. $\mu_{i,el}$, as before, represents the unknown density on Γ_i for the elastance problem and

$$u(\mathbf{x}) = u_{inc}(\mathbf{x}) + u_{sc}(\mathbf{x}) + u_\infty = S_\Gamma(\mu_{el} + \sigma_{el})(\mathbf{x}) + u_\infty . \qquad (113)$$

We then solve

$$\left(\frac{1}{2}I + K + L \right) \mu_{el} = - \left(\frac{1}{2}I + K \right) \sigma_{el}, \qquad (114)$$

where u_∞ is the potential at ∞ computed in the capacitance problem, and the operators K and L are described in section 2.5. This is a small modification of the representation presented in section 2.2 to account for the potential at ∞. After solving for μ_{el}, we may check the accuracy with which u in equation 113 equals the potential ϕ_j on Γ_j, the potentials prescribed in the original capacitance problem.

4.1.1 Two disc test

We first consider the case of two unit discs separated by a distance d. This is useful because the exact solution is known and because we wish to study the physical ill-conditioning of the problem as $d \to 0$.
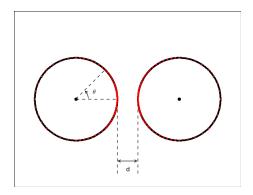
Figure 2: Discretization of the discs for Elastance example.

In the context of Fig. 2, we set $u|_{\Gamma_i} = \phi_i$ for $i = 1, 2$ (where $i = 1$ corresponds to the left disc), with $\phi_1 = 0.209$ and $\phi_2 = -0.123$. We consider $d = 0.5, 0.05, 0.005$.

We use a Nyström discretization, based on subdivision of the boundary into panels, with Gauss-Legendre nodes given on each panel. Let $\mathbf{s}_{i,j,l}$ denote the jth node on the ith panel on boundary component l. Let $\sigma_{i,j,l,el}, \mu_{i,j,l,el}$ denote the density evaluated at $\mathbf{s}_{i,j,l}$. We use a recently developed quadrature scheme, denoted by GLQBX (global + local quadrature by expansion) [33, 34] for evaluating the layer potential K in equation (114). This scheme is a robust extension of the QBX method of [35], guaranteed to yield high order accuracy even when boundaries are close-to-touching. We use an iterative GMRES-based solver to obtain to obtain μ_{el}, and iterate to a relative residue of 10^{-6}. As $d \to 0$, the problem becomes physically ill-conditioned, requiring an increasing number of iterations. To improve the rate of convergence, we use an L^2-based rescaling of the unknowns [36]. That is, we use $\mu_{el}^{scale} = \mu_{i,j,l,el}\sqrt{r_i}$ as unknowns, so that the discrete 2-norm approximates the L^2 norm where r_i is the length of panel i.

We iterate the following discretized linear system

$$D\left(\frac{1}{2}I + \tilde{K} + \tilde{L}\right)D^{-1}\mu_{el}^{scale} = -D\left(\frac{1}{2}I + \tilde{K}\right)\sigma_{el}, \qquad (115)$$

where $\tilde{K}$ and $\tilde{L}$ are discretized versions of K and L respectively, D is the diagonal operator described given by $D\mu_{el} = \mu_{el}^{scale}$.

In Fig. 3, we plot the net charge density $\sigma_{1,el} + \mu_{1,el}$ for the three different values of d. In Fig. 4, we plot the potential using the off-surface evaluation method of [37], whose development initially led to QBX. (The option of off-surface evaluation has been incorporated into our QBX software.)

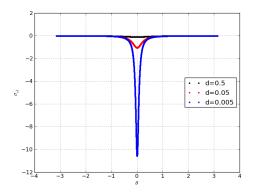From symmetry considerations, $\sigma_{2,el} + \mu_{2,el} = -(\sigma_{1,el} + \mu_{1,el})$.

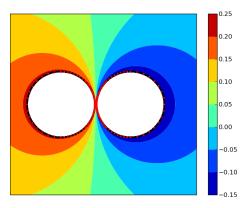Figure 3: Solution of integral equation for the elastance problem, $\sigma_{1,el} + \mu_{1,el}$ as a function of d.

Figure 4: Contour plot of u in the exterior of the two discs for $\phi_1 = 0.209$ and $\phi_2 = -0.123$ for $d = 0.05$.

As noted earlier, the two disc Dirichlet problem has an analytic solution. For this, suppose that the left disc is centered at $\mathbf{x}_1^c = \left(-1 - \frac{d}{2}, 0\right)$, that the right disc at $\mathbf{x}_2^c = \left(1 + \frac{d}{2}, 0\right)$, and that the discs are held at constant potentials ϕ_1 and ϕ_2. Then, the exterior potential is given by

$$u_{ex}\left(\mathbf{x}\right) = -\frac{v_1}{2\pi} \log\left(\frac{|\mathbf{x} - (\alpha, 0)|}{|\mathbf{x} + (\alpha, 0)|}\right) + v_2 \tag{116}$$

where

$$\alpha = \sqrt{d + \frac{d^2}{4}}, \quad v_1 = \pi \frac{(\phi_2 - \phi_1)}{\log\left(\frac{|\mathbf{x}_0 + (\alpha, 0)|}{|\mathbf{x}_0 - (\alpha, 0)|}\right)}, \quad v_2 = 0.5\left(\phi_1 + \phi_2\right) \tag{117}$$

25

with $\mathbf{x}_0 = \left(\frac{d}{2}\right)$. For each value of d, we compute the charge q_1 (since $q_2 = -q_1$), the iteration count for the elastance problem $n_{it,el}$, and the relative $\mathbb{L}^2$ error of the potential on boundary Γ_i given by $e_i = \sqrt{\frac{\int_{\Gamma_i} |u - u_{ex}|^2 \, ds_\mathbf{x}}{\int_{\Gamma_i} |u_{ex}|^2 \, ds_\mathbf{x}}}$. We emphasize again that this is *not* just a test of backward stability for the elastance solver, since we are solving two different boundary value problems.

d	q_1	$n_{it,el}$	e_1	e_2
0.5	-0.239487	4	$5.9\,10^{-8}$	$1.5\,10^{-7}$
0.05	-0.743917	8	$2.0\,10^{-5}$	$3.3\,10^{-5}$
0.005	-2.348079	15	$3.3\,10^{-5}$	$5.1\,10^{-5}$

Table 1: Summary of results for the capacitance and elastance problems with two discs.

4.1.2 Splash test

We repeat the test above with a more complicated geometry. We now consider 5 conductors D_j, whose boundaries Γ_j are parametrized by

$$x_j(\theta) = x_j^c + r_j(\theta)\cos(\theta + \beta_j) \tag{118}$$
$$y_j(\theta) = y_j^c + r_j(\theta)\sin(\theta + \beta_j) \tag{119}$$

where

$$r_j(\theta) = 1 + \sum_{k=1}^{12} a_{j,k}\sin(k\theta), \tag{120}$$

with the coefficients $a_{j,k}$ are uniformly chosen from $[0, 0.1]$ and prescribe an arbitrary potential on each of these objects.

We list here the parameters for defining the geometry and the exact solution in the previous section. The table of centers x_j^c, y_j^c, and β_j is given below.

	Γ_1	Γ_2	Γ_3	Γ_4	Γ_5
x_j^c	-1.2	1.2	0	-1.2	1.2
y_j^c	0	0	-2.2	-4.4	-4.4
β_j	π	0	$\frac{\pi}{8}$	$\frac{3\pi}{4}$	$-\frac{\pi}{4}$

Table 2: Parameters for setting up splash test for the Elastance and Mobility problems.

In the next table, we list the coefficients $a_{j,k}$ for $j = 1, 2 \dots 5$ and $k = 1, 2, \dots 12$.

Γ_1	Γ_2	Γ_3	Γ_4	Γ_5
0.012065	0.017038	0.070082	0.029959	0.012613
0.064385	0.041668	0.094629	0.069290	0.004017
0.006234	0.011991	0.046520	0.005102	0.07413
0.049028	0.022743	0.038905	0.067634	0.052361
0.030608	0.035266	0.043884	0.089215	0.084973
0.081641	0.10864	0.030143	0.097489	0.002916
0.099718	0.087338	0.084480	0.004693	0.081962
0.042460	0.096291	0.008018	0.055024	0.020443
0.076748	0.053323	0.069852	0.085238	0.069016
0.084684	0.040564	0.047617	0.070539	0.056950
0.016811	0.085034	0.015078	0.069771	0.051020
0.040454	0.016044	0.050553	0.051137	0.092286

Table 3: Coefficients $a_{j,k}$. For fixed j, the coefficients $a_{j,k}$ for Γ_j are listed in order of increasing k.

The prescribed potentials ϕ_j on Γ_j are given below, as well as the $\mathbb{L}^2$ norms for the errors in u, given by $e_i = \sqrt{\frac{\int_{\Gamma_i} |u - u_{ex}|^2 \, ds_{\mathbf{x}}}{\int_{\Gamma_i} |u_{ex}|^2 \, ds_{\mathbf{x}}}}$ on the boundary Γ_i. The potential u is computed after solving the elastance problem to see if we recover the exact values $u_{ex}|_{\Gamma_i} = \phi_i$.

j	1	2	3	4	5
ϕ_j	0.120625	0.643859	0.062342	0.490279	0.306079
e_j	$2.1\,10^{-5}$	$4.2\,10^{-6}$	$2.4\,10^{-5}$	$8.2\,10^{-6}$	$8.0\,10^{-6}$

Table 4: Prescribed potential on the boundary and the relative $\mathbb{L}^2$ error in potential on the boundary.

The elastance problem converged in 30 GMRES iterations, with a relative residual of 10^{-6}. In Fig. 5, we show a contour plot of u, with boundary values set to the ϕ_j.
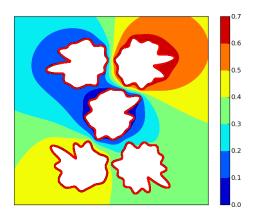
Figure 5: Contour plot of the potential u in the exterior of $\cup_j D_j$.

4.1.3 Application: Computing dielectric properties of nanocomposites

Nanocomposites are composite material consisting of nanoparticles in a host medium. Of particular interest are nanocomposites consisting of metallic particles in a homogeneous organic host due to their applications in transformation optics and high energy density storage materials. We shall treat the nanocomposite as a collection of nanoparticles which are perfect conductors in ambient space. Computing bulk dielectric properties of such materials as a function of shape, orientation and the volume fraction of these nanoparticles is of practical interest. Low frequency dielectric constants are typically determined experimentally using "capacitance" measurements. The dielectric constant is determined by measuring the voltage drop between two charged plates in the presence and absence of the nanocomposite. If the two conducting plates have charge $\pm Q$ and the measured potential difference is ΔV, then the "capacitance" of the configuration is computed as

$$\tilde{C} = \frac{Q}{\Delta V} \tag{121}$$

The potential drop, ΔV can be computed by solving an elastance problem.

Remark 8. *It should be noted that obtaingin $\tilde{C}$ in this manner is different from computing the mutual capacitance between the two plates for the given configuration of nanoparticles [38]. Experimentally one could have applied a potential difference between the two plates and measured the charge accumulated on them. However, to determine the mutual capacitance of this configuration numerically, one would need to know the potentials on each of the nanoparticles, and this data is not available.*

For fixed volume fraction, we carry out a two-dimensional version of the study in [38]. In particular, we study the effects of varying the number of particles and their aspect ratio. Let D_1 and D_2 with boundaries Γ_1 and Γ_2,

28

represent the capacitor plates. The boundaries Γ_1 and Γ_2 are shifted copies of a rounded bar γ parametrized by

$$x(s) = \begin{cases} 1.1\left(1 - \frac{2}{\pi}\left(e^{-100s^2} + s \cdot \text{erf}(10s)\right)\right) & s \in \left[-\frac{\pi}{2}, \frac{\pi}{2}\right] \\ -x(2\pi - s) & s \in \left(\frac{\pi}{2}, \frac{3\pi}{2}\right] \end{cases} \tag{122}$$

$$y(s) = \begin{cases} 0.1\text{erf}(7s) & s \in \left[-\frac{\pi}{2}, \frac{\pi}{2}\right] \\ y(2\pi - s) & s \in \left(\frac{\pi}{2}, \frac{3\pi}{2}\right] \end{cases} \tag{123}$$

The curve γ is discretized by sampling it at $s_k = -\frac{\pi}{2} + \pi(k - 0.5)/N$, $k = 1, 2, \ldots 2N$. We verify that the curve is well-resolved by studying the discrete Fourier coefficients of the sampled curve and choose N sufficiently large that the curve is approximated to at least the desired tolerance. More precisely, the boundaries Γ_1 and Γ_2 are parametrized by $(x(s), y(s) \pm 1.1)$ and discretized using 800 points each. For the nanoparticles, we use an $m \times 10$ lattice of elliptic inclusions, each of which has an area equal to $\frac{0.002}{m}$ and an aspect ratio A. They are centered at

$$\left(-0.9 + \frac{1.8(k - 1)}{10}, -0.9 + \frac{1.8(j - 1)}{m}\right) \quad j = 1, 2 \ldots m, \ k = 1, 2 \ldots 10. \tag{124}$$

The aspect ratio A is restricted to ensure that the nanoparticles do not overlap Each of these elliptical inclusions is discretized using an equispaced sampling of the central angle with 600 points each.
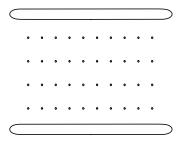

Figure 6: Capacitor plates with intervening nanoparticles. Here, there are $m = 4$ rows with aspect ratio set to $A = 0.5$.

In this case, we have a total of $10m + 2$ conductors whose boundaries are discretzed with $N_{pts} = 6000m + 1600$ points. We prescribe charges 1 and -1 on conductors Γ_1 and Γ_2, respectively, and assume the other $10m$ conductors are charge neutral. We measure the potential difference $\Delta V = V_1 - V_2$ where V_i is the potential on Γ_i, $i = 1, 2$ and compute the capacitance via equation (121) for various values of m, n and A. As before, we compute the layer potentials using a 6th order GLQBX scheme accelerated via an FMM, and iterate using GMRES until the relative residual in our computation is less than 10^{-6}.
Let $\tilde{C}_0$ be the capacitance in the absense of the nanocomposite (corresponding to

m	A	N_{pts}	N_{it}	t_{solve}	$\tilde{C}$
0	-	1600	8	0.4539	2.2949
1	0.25	7600	11	3.2965	2.3147
	0.5		8	2.2417	2.3073
	1.0		8	2.2907	2.3033
	2.0		8	2.2167	2.3013
	4.0		11	3.4305	2.3003
4	0.25	25600	11	11.5612	2.3191
	0.5		9	8.7257	2.3095
	1.0		7	7.2139	2.3047
	2.0		9	8.6497	2.3023
	4.0		10	10.1145	2.3012
16	0.25	97600	11	44.8332	2.3200
	0.5		9	33.6639	2.3099
	1.0		8	31.2122	2.3049
	2.0		9	33.5139	2.3024
	4.0		11	46.4239	2.3012

Table 5: Capacitance of nanocomposites. N_{it} is the number of GMRES iterations, and t_{solve} is the time taken to solve the elastance problem in seconds on a single CPU core.

$m = 0$). We plot below the percentage change in capacitance $100 \left(\tilde{C} - \tilde{C}_0 \right) / \tilde{C}_0$ as a function of m and A.
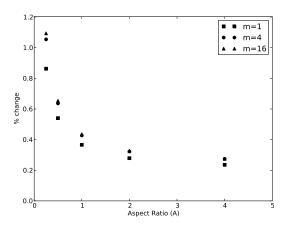

Figure 7: % change in $\tilde{C}$ as a function of m and A.

4.2 Mobility problem

We turn now to a test for our mobility representation. Given prescribed velocities for a set of rigid bodies, we solve the resistance problem and compute the

resulting forces and torques on them. We then use these forces and torques as input for the mobility problem and check that the velocity on the boundary of the rigid body is the prescribed rigid body motion. As before, this is a stringent test, since the integral equation for the resistance problem is *not* simply the inverse of the integral equation for the mobility problem.

We consider, as above, the domain exterior to N rigid bodies D_i, whose boundaries are given by Γ_i. We prescribe velocities $\mathbf{u} = \mathbf{v}_i + \omega_i (\mathbf{x} - \mathbf{x}_i^c)^\perp$ on Γ_i and, solve the resistance problem to compute the forces and torques on the rigid bodies D_i and also the velocity at ∞, $\mathbf{u}_\infty = \lim_{|\mathbf{x}| \to \infty} \mathbf{u}(\mathbf{x})$. We use these forces and torques as input for the mobility problem to compute the rigid body motions. Let $\boldsymbol{\rho}_{i,mob}$ denote the incident velocity field due to the forces and torques as described in section 3.2 and let $\boldsymbol{\mu}_{i,mob}$ represent the unknown density on Γ_i for the mobility problem. To summarize, we set

$$\mathbf{u}(\mathbf{x}) = \mathbf{u}_{inc}(\mathbf{x}) + \mathbf{u}_{sc}(\mathbf{x}) + \mathbf{u}_\infty = \mathcal{S}_\Gamma (\boldsymbol{\mu}_{mob}(\mathbf{x}) + \boldsymbol{\rho}_{mob}(\mathbf{x})) + \mathbf{u}_\infty, \quad (125)$$

and wish to solve

$$\left(\frac{1}{2} \mathbf{I} + \mathcal{K} + \mathbf{L} \right) \boldsymbol{\mu}_{mob} = - \left(\frac{1}{2} \mathbf{I} + \mathcal{K} \right) \boldsymbol{\rho}_{mob}, \quad (126)$$

where $\boldsymbol{\mu}_{mob} = (\boldsymbol{\mu}_{1,mob}, \boldsymbol{\mu}_{2,mob})$, $\boldsymbol{\rho}_{mob} = (\boldsymbol{\rho}_{1,mob}, \boldsymbol{\rho}_{2,mob})$, $\mathbf{u}_\infty$ is the velocity at ∞ computed in the resistance problem, and the operators $\mathcal{K}$ and $\mathbf{L}$ are described in section 3.5. This is a small modification of the representation presented in section 3.2 to account for the velocity at ∞. After solving for $\boldsymbol{\mu}_{mob}$, we verify that $\mathbf{u}$ in equation (125) is the original rigid body motion.

4.2.1   Two discs

We first test the mobility representation in the exterior of two discs, with the same geometry is above, in section 4.1.1. However, we use a finer discretization to resolve the more singular densities incurred in the mobility problem.
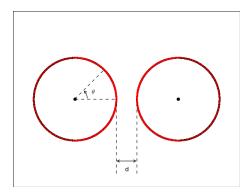

Figure 8: Discretization of the discs for Mobility example.

Refering to Fig. 8, we set $\mathbf{u}|_{\Gamma_i} = \mathbf{v}_i + \omega_i (\mathbf{x} - \mathbf{x}_i^c)^{\perp}$ for $i = 1, 2$ ($i =$ corresponds to the disc on the left), where we set $\mathbf{v}_1 = (2.09, 1.00)$, $\mathbf{v}_2 = (-1.034, 0.254)$, $\omega_1 = 0.12$ and $\omega_2 = 0.33$. We again test the problem for $d = 0.5, 0.05, 0.005$.
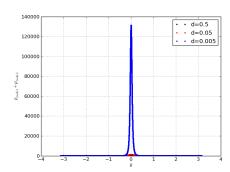
As above, we use a Nyström discretization with Gauss-Legendre panels. $\mathbf{s}_{i,j,l}$ denotes the jth Gauss-Legendre node on panel i on boundary l. Let $\boldsymbol{\rho}_{i,j,l,mob}, \boldsymbol{\mu}_{i,j,l,mob}$ denote the densities at $\mathbf{s}_{i,j,l}$. We use the GLQBX quadrature scheme for evaluating the layer potential, $\frac{1}{2}\mathbf{I} + \mathcal{K}$ in equation (126). We use an iterative GMRES-based solver to obtain $\boldsymbol{\mu}_{mob}$, with a relative residual tolerance of 10^{-6}. The physical conditioning increases as $d \to 0$, requiring a large number of iterations. To improve the rate of convergence of GMRES, we use L^2 weighting for the unknowns [36]. That is, we use $\boldsymbol{\mu}_{mob}^{scale} = \boldsymbol{\mu}_{i,j,l,mob}\sqrt{r_i}$ as unknowns.

We solve the following linear system

$$ D\left(\frac{1}{2}\mathbf{I} + \tilde{\mathcal{K}} + \tilde{\mathbf{L}}\right) D^{-1}\boldsymbol{\mu}_{mob}^{scale} = -D\left(\frac{1}{2}\mathbf{I} + \tilde{\mathcal{K}}\right)\boldsymbol{\rho}_{mob}, \tag{127} $$

where $\tilde{\mathcal{K}}$ and $\tilde{\mathbf{L}}$ are discretized versions of $\mathcal{K}$ and $\mathbf{L}$ respectively, and D is the diagonal operator given by $D\boldsymbol{\mu}_{mob} = \boldsymbol{\mu}_{mob}^{scale}$.

We plot below the net surface traction $\boldsymbol{\rho}_{1,mob} + \boldsymbol{\mu}_{1,mob}$ and a quiver plot of the velocity field in the exterior of the two discs for $d = 0.05$ (Figs. 9 and 10). From symmetry considerations, $\boldsymbol{\rho}_{2,mob} + \boldsymbol{\mu}_{2,mob} = -\left(\boldsymbol{\rho}_{1,mob} + \boldsymbol{\mu}_{1,mob}\right)$.
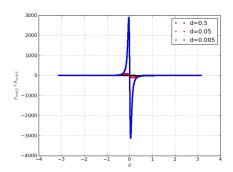

Figure 9: Integral equation solution for the mobility problem: $\rho_{1,1,mob} + \mu_{1,1,mob}$ (left) and $\rho_{2,1,mob} + \mu_{2,1,mob}$ (right) as a function of θ for $d = 0.5, 0.05, 0.005$
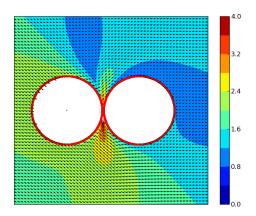
Figure 10: Quiver plot of **u** and contour plot of $|\mathbf{u}|$ in the exterior of the two discs.

For each value of d, we compute the forces and torques $F_{1,1}, F_{2,1}, T_1, T_2$ (since $\mathbf{F}_2 = -\mathbf{F}_1$), the iteration count for the mobility problem, n_{it}, and the relative $\mathbb{L}^2$ error of the velocity on both the boundaries Γ_1 and Γ_2 given by $e_i = \sqrt{\frac{\int_{\Gamma_i} |\mathbf{u} - \mathbf{u}_{ex}|^2 \, ds_{\mathbf{x}}}{\int_{\Gamma_i} |\mathbf{u}_{ex}|^2 \, ds_{\mathbf{x}}}}$. This is again a nontrivial test of our solvers, as we enforce boundary conditions on the fluid stress here, not the velocity **u**.

d	$F_{1,1}$	$F_{2,1}$	T_1	T_2	n_{it}	e_1	e_2
0.5	27.180434	-6.575686	-1.496082	1.494675	7	$8.8\,10^{-8}$	$1.8\,10^{-5}$
0.05	499.08688	-15.202716	-11.159661	-4.859692	19	$5.1\,10^{-6}$	$8.5\,10^{-6}$
0.005	14653.544	-40.877338	-42.867299	-24.078713	60	$1.0\,10^{-6}$	$2.2\,10^{-6}$

Table 6: Summary of results for two discs test for resistance and mobility problems.

4.2.2 Splash test

We repeat the test above in a more complicated geometry, but consider 5 bodies D_j, whose boundaries Γ_j are parametrized as

$$x_j\,(\theta) = x_j^c + r_j(\theta)\cos(\theta + \beta_j) \tag{128}$$

$$y_j\,(\theta) = y_j^c + r_j(\theta)\sin(\theta + \beta_j) \tag{129}$$

where

$$r_j(\theta) = 1 + \sum_{k=1}^{12} a_{j,k}\sin\,(k\theta) \tag{130}$$

where the parameters $a_{j,k}$, x_j^c and y_j^c are the described in section 4.1.2.

33

The prescribed velocities $\mathbf{v}_j = (v_{1,j}, v_{2,j})$ and ω_j on Γ_j are given below, along with the $\mathbb{L}^2$ norm in the error in $\mathbf{u}$, given by $e_i = \sqrt{\frac{\int_{\Gamma_i} |\mathbf{u} - \mathbf{u}_{ex}|^2 \, ds_{\mathbf{x}}}{\int_{\Gamma_i} |\mathbf{u}_{ex}|^2 \, ds_{\mathbf{x}}}}$ on the boundary Γ_i, after solving the mobility problem is listed below where $\mathbf{u}_{ex}|_{\Gamma_i} = \mathbf{v}_i + \omega_i (\mathbf{x} - \mathbf{x}_i^c)^\perp$.

j	1	2	3	4	5
$v_{1,j}$	-0.379375	-0.009720	0.497180	0.346837	-0.197527
$v_{2,j}$	0.143846	-0.193921	-0.075401	-0.331891	0.273004
ω_j	-0.437658	0.316414	0.267477	-0.095456	-0.184353
e_j	$1.8 \, 10^{-5}$	$2.5 \, 10^{-5}$	$1.1 \, 10^{-5}$	$1.3 \, 10^{-5}$	$1.3 \, 10^{-5}$

Table 7: Prescribed velocity on the boundary and the relative $\mathbb{L}^2$ error in velocity on the boundary after solving the resistane and mobility problems.

The mobilitiy problem converged in 71 GMRES iterations to a relative tolerance of 10^{-6}. We show a quiver plot for the velocity $\mathbf{u}$ corresponding to the above prescribed value of velocity on the boundary $\mathbf{u}|_{\Gamma_j}$. The background is a contour plot of the magnitude $|\mathbf{u}|$ in the exterior of the $\cup_j D_j$ (Fig. 11).
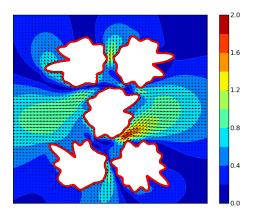

Figure 11: Quiver plot of $\mathbf{u}$ superimposed on contour plot of $|\mathbf{u}|$ in the exterior of $\cup_j D_j$.

5 Conclusions

We have derived a new, physically motivated integral formulation for the elastance problem in exterior domains. The analogous physical reasoning yields a new derivation of an integral equation developed earlier by Kim and Karrila for the mobility problem [27]. Discretization of the resulting integral equations using the quadrature scheme GLQBX [33, 34] permits high order accuracy to

be obtained in complex geometry, including the interaction of close-to-touching boundary components. The resulting linear systems can be solved iteratively using GMRES and the necessary matrix-vector multiplications can be accelerated using the fast multipole method. If N denotes the number of points used in the discretization of the physical boundaries, the total cost scales linearly with N. We are currently working on the extension of our scheme to closed or periodic systems and to problems in three dimensions.

Acknowledgments

References

[1] W. R. Smythe, *Static and Dynamic Electricity.* McGraw Hill, New York, 1975.

[2] J. D. Jackson, *Classical Electrodynamics.* Wiley, New York, 1975.

[3] S. Kapur and D. E. Long, "Large-scale capacitance calculation," in *in Proc. 37th Design Automation Conference*, pp. 744–749, 2000.

[4] Y. C. Pan, L. X. Wan, and W. C. Chew, "A fast multipole method based calculation of the capacitance matrix in a stratified medium," in *Antennas and Propagation Society International Symposium, 2000. IEEE*, vol. 4, pp. 1876–1879 vol.4, July 2000.

[5] J. Tausch and J. White, "Second-kind integral formulations of the capacitance problem," *Advances in Computational Mathematics*, vol. 9, no. 2, pp. 217–232, 1998.

[6] W. T. Weeks, "Calculation of coefficients of capacitance of multiconductor transmission lines in the presence of a dielectric interface," *Microwave Theory and Techniques, IEEE Transactions on*, vol. 18, pp. 35–43, Jan 1970.

[7] A. M. Chang and J. C. Chen, "The Kondo effect in coupled-quantum dots," *Reports on Progress in Physics*, vol. 72, p. 096501, Sept. 2009.

[8] W. G. van der Wiel, S. De Franceschi, J. M. Elzerman, T. Fujisawa, S. Tarucha, and L. P. Kouwenhoven, "Electron transport through double quantum dots," *Reviews of Modern Physics*, vol. 75, pp. 1–22, 2003.

[9] J. Koch, T. Yu, J. Gambetta, A. Houck, D. Schuster, J. Majer, A. Blais, M. Devoret, S. Girvin, and R. Schoelkopf, "Charge-insensitive qubit design derived from the cooper pair box," *Physical Review A*, vol. 76, p. 042319, Oct. 2007.

[10] S. Delong, F. B. Usabiaga, R. Delgado-Buscalioni, B. E. Griffith, and A. Donev, "Brownian Dynamics without Green's Functions," *arXiv:1401.4198v2*, 2014.

[11] K. Ichiki and J. F. Brady, "Many-body effects and matrix inversion in low-Reynolds-number hydrodynamics," *Physics of Fluids*, vol. 13, no. 1, p. 350, 2001.

[12] S. Kim and S. Karrila, *Microhydrodynamics: Principles and Selected Applications*. Butterworth - Heinemann series in chemical engineering, Dover Publications, 2005.

[13] C. Pozrikidis, *Boundary Integral and Singularity Methods for Linearized Viscous Flow*. Cambridge Texts in Applied Mathematics, Cambridge University Press, 1992.

[14] W. C. Chew, J.-M. Jin, E. Michielssen, and J. Song, *Fast and Efficient Algorithms in Computational Electromagnetics*. Artech House, Boston, 2001.

[15] Y. Liu, *Fast Multipole Boundary Element Method: Theory and Applications in Engineering*. Cambridge University Press, New York, 2009.

[16] L. Greengard and V. Rokhlin, "A new version of the fast multipole method for the Laplace equation in three-dimensions," *Acta Numerica*, vol. 6, pp. 229–269, 1997.

[17] N. Nishimura, "Fast multipole accelerated boundary integral equation methods," *Appl. Mech. Rev.*, vol. 55, pp. 299–324, 2002.

[18] A. Greenbaum, L. Greengard, and G. McFadden, "Laplace's equation and the Dirichlet-Neumann map in multiply connected domains," *Journal of Computational Physics*, vol. 105, pp. 267–278, 1993.

[19] J. Helsing and E. Wadbro, "Laplace's equation and the Dirichlet-Neumann map: a new mode for Mikhlin's method," *Journal of Computational Physics*, vol. 202, pp. 391–410, Jan. 2005.

[20] S. Mikhlin, *Integral equations and their applications to certain problems: in mechanics, mathematical physics and technology*. International series of monographs in pure and applied mathematics, Macmillan, 1964.

[21] K. Nabors, F. T. Korsmeyer, F. T. Leighton, and J. White, "Preconditioned, adaptive, multipole-accelerated iterative methods for three-dimensional first-kind integral equations of potential theory," *SIAM Journal on Scientific Computing*, vol. 15, pp. 713–735, 1994.

[22] G. Biros, L. Ying, and D. Zorin, "A fast solver for the Stokes equations with distributed forces in complex geometries," *Journal of Computational Physics*, vol. 193, pp. 317–348, 2003.

[23] L. Greengard, M. C. Kropinski, and A. Mayo, "Integral equation methods for Stokes flow and isotropic elasticity in the plane," *Journal of Computational Physics*, vol. 125, pp. 403–414, 1993.

[24] H. Power and G. Miranda, "Second kind integral equation formulation of Stokes flows past a particle of arbitrary shape," *SIAM Journal on Applied Mathematics*, vol. 47, pp. 689–698, 1987.

[25] R. Cortez, L. Fauci, and A. Medovikov, "The method of regularized Stokeslets in three dimensions: Analysis, validation, and application to helical swimming," *Physics of Fluids*, vol. 17, no. 3, p. 031504, 2005.

[26] M. Kropinski, "Integral equation methods for particle simulations in creeping flows," *Computers & Mathematics with Applications*, vol. 38, pp. 67–87, Sept. 1999.

[27] S. J. Karrila and S. Kim, "Integral equations of the second kind for Stokes flow: direct solution for physical variables and removal of inherent accuracy limitations," *Chemical engineering communications*, vol. 82, no. 1, pp. 123–161, 1989.

[28] L. Af Klinteberg and A.-K. Tornberg, "Fast Ewald summation for Stokesian particle suspensions," *International Journal for Numerical Methods in Fluids*, vol. 76, no. 10, pp. 669–698, 2014.

[29] R. Kress, *Linear Integral Equations.* Applied Mathematical Sciences, Springer New York, 1999.

[30] R. Guenther and J. Lee, *Partial Differential Equations of Mathematical Physics and Integral Equations.* Prentice Hall, 1988.

[31] J. Sifuentes, Z. Gimbutas, and L. Greengard, "Randomized methods for rank-deficient linear systems," *arXiv:1401.3068*, 2014.

[32] R. Finn and W. Noll, "On the uniqueness and non-existence of Stokes flows," *Archive for Rational Mechanics and Analysis*, vol. 1, no. 1, pp. 97–106, 1957.

[33] M. Rachh, *Integral equation methods for problems in electrostatics, elastostatics and viscous flow.* 2015. Thesis (Ph.D.)–New York University.

[34] M. Rachh, A. Klöckner, and M. O'Neil, "A hybrid version of QBX (quadrature by expansion) for the evaluation of layer potentials in close-to-touching geometries," *in preparation.*

[35] A. Klöckner, A. Barnett, L. Greengard, and M. O'Neil, "Quadrature by expansion: A new method for the evaluation of layer potentials," *Journal of Computational Physics*, vol. 252, pp. 332–349, Nov. 2013.

[36] J. Bremer and V. Rokhlin, "Efficient discretization of Laplace boundary integral equations on polygonal domains," *Journal of Computational Physics*, vol. 229, no. 7, pp. 2507–2525, 2010.

[37] A. Barnett, "Evaluation of layer potentials close to the boundary for Laplace and Helmholtz problems on analytic planar domains," *SIAM J. Sci. Comput.*, vol. 36, pp. A427–A451, 2014.

[38] X. Zheng, J. Fontana, M. Pevnyi, M. Ignatenko, S. Wang, R. Vaia, and P. Palffy-Muhoray, "The effects of nanoparticle shape and orientation on the low frequency dielectric properties of nanocomposites," *Journal of Materials Science*, vol. 47, no. 12, pp. 4914–4920, 2012.